Table 2. Frequency monitoring of the number of survivin-2B80-88 peptide tetramer-positive CTLs in cancer patients treated with IFNα alone

Patient no.	Tumor	Age/sex	Number of treatment	Tetramer stainingt		ELISPOT‡	
				Pre/post	% Increase	Pre/post	% Increase
1	Colon	60/M	3	1/0	0.0	111/75	67.6
2	Colon	63/M	4	11/9	81.8	44/20	45.5
3	Colon	77/F	2	13/3	23.1	26/40	153.8

†CTL frequency before and after treatment with IFNα alone in patients was assessed with an HLA-A24-restricted survivin-2B80-88 (AYACNTSTL) peptide tetramer. An HLA-A24-restricted HIV peptide (RYLRDQQLL) tetramer was used as a negative control. The number of survivin-2B80-88 peptide tetramer-positive but HIV peptide-negative CTLs in 10^4 CD8 T cells is shown. ‡γ-Interferon (IFNγ) secretion of pre and post IFNα treatmnet were assesed with ELISPOT assay using T2-A24 cells pulsed with survivin2B80-88 peptide. The number of spots in 5×10^3 CD8 T cells are shown. IFNα, α-interferon.

detects naive T cells, memory T cells, and activated CTLs. The ELISPOT assay detects more the functional aspects of T cells by IFNγ release, therefore, ELISPOT detects memory T cells and CTLs. In this study, the tetramer-positive cases are also positive in the ELISPOT study. Therefore, these results indicate that memory T cells and CTLs can be effectively induced by this peptide vaccination protocol.

In this present study, we also assessed evidence concerning the extent to which peptide-specific CTL responses in pancreatic cancer patients treated with peptide vaccines could occur at the single-cell level. To assess this, CTLs of patients were sorted to the single-cell level, and we confirmed that each CTL obtained from vaccinated patients was indeed peptide-specific in the context of the expression of HLA-A24.

Type-I interferons such as IFNα are known to work in various immunological manners to activate T cell responses.[18–25] The maturation of DCs and their effect on the expression of HLA molecules seems to be the main action of this cytokine. Although we could not actually compare these features of patients' DCs and primary pancreatic tumor tissues before and after treatment with IFNα, the obvious enhancement of CTL responses and improvement of clinical responses in our previous and current studies favors the two main actions described above. These observations strongly suggest that the action of IFNα is remarkable from the aspect of being an immunogenic enhancer for human cancer peptide vaccines.

It is widely known that IFNα is involved in DC maturation and activation.[18,21] This particular cytokine is also potent for increasing the expression of MHC class I molecules.[26–29] Indeed, our previous study of the expression of HLA class I molecules in pancreatic cancer indicated that many tumor tissues heterogeneously expressed such molecules, with some tumor cells showing high expression, whereas others had only weak expression. Interferon-α is presumed to actually enhance their expression even in those tumor tissues with weak expression. Moreover, because tumor patients generally show overt expression of survivin protein in their tumor tissues and, although in small numbers, survivin-2B peptide-specific T cells in peripheral blood, it is considered that IFNα alone may increase the frequency of these T cells in peripheral blood as well. These features of this particular cytokine lead to the possibility that treatment with IFNα alone could result in, at least to some extent, certain immunological and clinical effects of survivin-2B peptide-specific T cells in tumor-bearing patients. However, we analyzed three colon cancer patients, and our data strongly suggested that there was no increase of these T cells as assessed by tetramer and ELISPOT analyses.

Taken together, our results highly suggest that the vaccination protocol with survivin-2B80-88 plus IFA and IFNα is very effective for pancreatic and colon cancers, and that this protocol might be useful as a standard, general immunotherapy modality for human cancers. However, further clinical studies involving many patients are necessary in order to consolidate the immunotherapeutic benefit of this vaccination protocol.

Acknowledgments

This work was supported by Grants-in-Aid for Scientific Research from the Ministry of Education, Culture, Sports, Science and Technology of Japan (grant nos 16209013, 17016061, and 15659097), and for Practical Application Research from the Japan Science and Technology Agency and for Cancer Research (15-17 and 19-14) from the Ministry of Health, Labor and Welfare of Japan. We are also very grateful for grants from the Akiyama Life Science Foundation and the Ono Foundation, and for continuous support providing study samples by the Hokkaido Red Cross Blood Center.

Disclosure Statement

The authors have no conflict of interest.

References

1 Hirohashi Y, Torigoe T, Inoda S *et al.* The functioning antigens; beyond just as the immunologic targets. *Cancer Sci* 2009; **100**: 798–806.
2 Sato N, Hirohashi Y, Tsukahara T *et al.* Molecular pathologic approaches to human tumor immunology. *Pathol Int* 2009; **59**: 205–17.
3 Rosenberg SA, Yang JC, Restifo NP. Cancer immunotherapy: moving beyond current vaccines. *Nature Med* 2004; **10**: 909–15.
4 Tsukahara T, Torigoe T, Tamura Y, Kawaguchi S, Wada T, Sato N. Antigenic peptide vaccination: provoking immune response and clinical benefit for cancer. *Curr Immunol Rev* 2008; **4**: 235–41.
5 Rosenberg SA. A new era for cancer immunotherapy based on the genes that encode cancer antigens. *Immunity* 1999; **10**: 281–7.
6 Andersen MH, Becker JC, Straten P. Regulators of apoptosis: suitable targets for immune therapy of cancer. *Nat Rev Drug Discov* 2005; **4**: 399–409.
7 Van der Bruggen P, Traversari C, Chomez P *et al.* A gene encoding an antigen recognized by cytolytic T lymphocytes on a human melanoma. *Science* 1991; **254**: 1643–7.
8 Kameshima H, Tsuruma T, Torigoe T *et al.* Immunogenic enhancement and clinical effect by type-I interferon of anti-apoptotic protein, survivin-derived peptide vaccine, in advanced colorectal cancer patients. *Cancer Sci* 2011; **102**: 1181–7.
9 Tsuruma T, Hata F, Torigoe T *et al.* Phase I clinical study of anti-apoptosis protein, survivin-derived peptide vaccine therapy for patients with advanced or recurrent colorectal cancer. *J Transl Med* 2004; **2**: 19–29.
10 Tsuruma T, Iwayama Y, Ohmura T *et al.* Clinical and immunological evaluation of anti-apoptosis protein, survivin-derived peptide vaccine in phase I clinical study for patients with advanced or recurrent breast cancer. *J Transl Med* 2008; **6**: 24–35.
11 Kawaguchi S, Wada T, Ida K *et al.* Phase Ivaccination trial of SYT-SSX junction peptide in patients with disseminated synovial sarcoma. *J Transl Med* 2005; **3**: 1–9.
12 Honma I, Kitamura H, Torigoe H *et al.* Phase I clinical study of anti-apoptosis protein survivin-derived peptide vaccination for patients with advanced or recurrent urothelial cancer. *Cancer Immunol Immunother* 2009; **58**: 1801–7.

doi: 10.1111/cas.12046

13 Torigoe T, Asanuma H, Nakazawa E *et al.* Establishment of a monoclonal anti-pan HLA class I antibody suitable for immunostaining of formalin-fixed tissue: unusually high frequency of down-regulation in breast cancer tissues. *Pathol Int* 2012; **62**: 303–8.
14 Coulie PG, Karanikas V, Lurquin C. Cytolytic T-cell response of cancer patients vaccinated with a MAGE antigen. *Immunol Rev* 2002; **188**: 33–42.
15 Nagaraj S, Pisarev V, Kinarsky L *et al.* Dendritic cell-based full-length survivin vaccine in treatment of experimental tumors. *J Immunother* 2007; **30**: 169–79.
16 Hirohashi Y, Torigoe T, Maeda A *et al.* An HLA-A24-restricted cytotoxic T lymphocyte epitope of a tumor-associated protein, survivin. *Clin Cancer Res* 2002; **8**: 1731–9.
17 Idenoue S, Hirohashi Y, Torigoe T *et al.* A potent immunogenic general cancer vaccine that targets survivin, an inhibitor of apoptosis proteins. *Clin Cancer Res* 2005; **11**: 1474–82.
18 Le Bon A, Etchart N, Rossmann C *et al.* Cross-priming of $CD8^+$ T cells stimulated by virus-induced type I interferon. *Nat Immunol* 2003; **4**: 1009–15.
19 Dikopoulos N, Bertoletti A, Kroeger A, Hauser H, Schirmbeck R, Reimann J. Type I IFN negatively regulates $CD8^+$ T cell responses through IL-10-producing $CD4^+$ T regulatory 1 cells. *J Immunol* 2005; **174**: 99–109.
20 Di Pucchio T, Pilla L, Capone I *et al.* Immunization of stage IV melanoma patients with Melan-A/MART-1 and gp100 peptides plus IFN-α results in the activation of specific $CD8^+$ T cells and monocyte/dendritic cell precursors. *Cancer Res* 2006; **66**: 4943–51.
21 Gigante M, Mandic M, Wesa AK *et al.* Interferon-alpha (IFN-alpha)-conditioned DC preferentially stimulate type-1 and limit Treg-type *in vitro* T-cell responses from RCC patients. *J Immunother* 2008; **31**: 254–62.
22 Schwaab T, Schwarzer A, Wolf B *et al.* Clinical and immunologic effect of intranodal autologous tumor lysate-dendritic cell vaccine with Aldesleukim (interleukin 2) and IFN-α2a therapy in metastatic renal cell carcinoma patients. *Clin Cancer Res* 2009; **15**: 4986–92.
23 Trepiakas R, Pedersen AE, Met O, Svane IM. Addition of interferon-alpha to a standard maturation cocktail induces CD38 up-regulation and increases dendritic cell function. *Vaccine* 2009; **27**: 2213–9.
24 Shimizu K, Kurosawa Y, Taniguchi M, Steinman RM, Fujii S. Cross-presentation of glycolipid from tumor cells loaded with α-galactsylceramide leads to potent and long-lived T cell mediated immunity via dendritic cells. *J Exp Med* 2007; **204**: 2641–53.
25 Badovinac VP, Messingham KN, Jabbari A, Haring JS, Harty JT. Accelerated $CD8^+$ T-cell memory and prime-boost response after dendritic-cell vaccination. *Nature Med* 2005; **11**: 748–56.
26 Spadaro F, Lapenta C, Donati S *et al.* IFN−α enhances cross-presentation in human dendritic cells by modulating antigen survival, endocytic routing, and processing. *Blood* 2012; **119**: 1407–17.
27 Truong P, Heydari S, Garidou L, McGavern DB. Persistent viral infection elevates central nervous system MHC class I through chronic production of interferons. *J Immunol.* 2009; **183**: 3895–905.
28 Garrido F, Cabrera T, Aptsiauri N. Hard and soft lesions underlying the HLA class I alterations in cancer cells; implications for immunotherapy. *Int J Cancer* 2010; **127**: 249–56.
29 Khallouf H, Marten A, Serba S *et al.* 5-Fluorouracil and interferon-α immunotherapy enhances immunogenicity of murine pancreatic cancer through upregulation of NKG2S ligands and MHC class I. *J Immunother* 2012; **35**: 245–53.

Cancer Science
The official journal of the Japanese Cancer Association JCA

Prostate cancer stem-like cells/cancer-initiating cells have an autocrine system of hepatocyte growth factor

Sachiyo Nishida,[1,2] Yoshihiko Hirohashi,[1,4] Toshihiko Torigoe,[1,4] Ryuta Inoue,[1,2] Hiroshi Kitamura,[2] Toshiaki Tanaka,[2] Akari Takahashi,[1] Hiroko Asanuma,[3] Naoya Masumori,[2] Taiji Tsukamoto[2] and Noriyuki Sato[1]

Departments of [1]Pathology; [2]Urology; [3]Surgical Pathology, Sapporo Medical University School of Medicine, Sapporo, Japan

(Received August 8, 2012/Revised December 31, 2012/Accepted January 4, 2013/Accepted manuscript online January 15, 2013/Article first published online February 17, 2013)

Prostate cancer cells include a small population of cancer stem-like cells (CSCs)/cancer-initiating cells (CICs) that have roles in initiation and progression of the cancer. Recently, we isolated prostate CSCs/CICs as aldehyde dehydrogenase 1-highh (ALDH1^{high}) cells using the ALDEFLUOR assay; however, the molecular mechanisms of prostate CSCs/CICs are still elusive. Prostate CSCs/CICs were isolated as ALDH1^{high} cells using the ALDEFLUOR assay, and the gene expression profiles were analyzed using a cDNA microarray and RT-PCR. We found that prostate CSCs/CICs expressed higher levels of growth factors including hepatocyte growth factor (HGF). Hepatocyte growth factor protein expression was confirmed by enzyme linked immunosorbent assay and Western blotting. On the other hand, c-MET HGF receptor was expressed in both CSCs/CICs and non-CSCs/CICs at similar levels. Hepatocyte growth factor and the supernatant of myofibloblasts derived from the prostate augmented prostasphere formation *in vitro*, and prostasphere formation was inhibited by an anti-HGF antibody. Furthermore, c-MET gene knockdown by siRNA inhibited the prostasphere-forming ability *in vitro* and tumor-initiating ability *in vivo*. Taken together, the results indicate that HGF secreted by prostate CSCs/CICs and prostate myofibroblasts has a role in the maintenance of prostate CSCs/CICs in an autocrine and paracrine fashion. (*Cancer Sci* 2013; 104: 431–436)

Prostate cancer is one of the common and lethal cancers in males. Although there are some curative treatments for early-stage prostate cancer, there is no effective treatment for advanced metastatic prostate cancer. Cancer stem-like cells (CSCs)/cancer-initiating cells (CICs) have high tumor-initiating ability and are resistant to chemotherapy and radiotherapy, and CSCs/CICs are therefore thought to be responsible for cancer recurrence after treatment and for distant metastasis.[1,2]

Prostate cancer contains a small population of CSCs/CICs, and we previously described the successful isolation of prostate CSCs/CICs from the human prostate carcinoma cell line 22Rv1 by using aldehyde dehydrogenase (ALDH) activity.[3] In addition, we isolated prostate CSC/CIC-specific genes, including *HGF* and *IGF1*, by microarray screening and RT-PCR analysis. In a physiological condition, hepatocyte growth factor (HGF) is secreted by mesenchymal cells and promotes epithelial cell growth in a paracrine fashion. However, signaling of HGF and its receptor c-MET is activated in cancer cells and is related to cancer cell growth, cell motility and matrix invasion, and HGF/c-MET signaling can therefore be a reasonable target of cancer therapy.[4] In this study, we confirmed HGF protein secretion from prostate CSCs/CICs, and we investigated the HGF/c-MET signaling function in maintenance of prostate CSCs/CICs.

Materials and Methods

Cell culture and ALDEFLUOR assay. The human prostate cancer cell line 22Rv1 was obtained from American Type Culture Collection (ATCC, Manassas, VA, USA), and the cells were cultured in DMEM (Life Technologies, Grand Island, NY, USA) supplemented with 10% FCS. Prostate myofibroblast cells (WPMY-1) were purchased from ATCC and were cultured in DMEM supplemented with 5% of FCS. The cells were kept in a 37°C incubator with humidified air and 5% CO_2. The culture medium was changed twice a week. ALDEFLUOR assay was performed as described previously.[3] ALDH1^{high} and ALDH1^{low} cells were defined as those in the previous report.[3]

RNA preparation and reverse transcription-polymerase chain reaction. Isolation of total RNA and RT-PCR analysis were performed as described previously.[3] Primer pairs used for RT-PCR analysis were 5′-GGGCTGAAAAGATTGGATCA-3′ and 5′-TTGTATTGGTGGGTGCTTCA-3′ for *HGF* with an expected PCR product size of 245 base pairs (bp), 5′-CAGGC AGTGCAGCATGTAGT-3′ and 5′-GATGATTCCCTCGGTCA GAA-3′ for *MET* (hepatocyte growth factor receptor) with an expected PCR product size of 201 bp, and 5′-ACCACAGTC CATGCCATCAC-3′ and 5′-TCCACCACCCTGTTGCTGTA-3′ for *glyceraldehyde-3-phosphate dehydrogenase* (GAPDH) with an expected product size of 452 bp.

Enzyme-linked immunosorbent assay. Sorted ALDH1^{high} and ALDH1^{low} cells (10 000 cells each) were incubated in 150 μL DMEM + 10% FCS media in each well of a 96-well plate for 48 h. Enzyme linked immunosorbent assay was performed for detection of HGF in each cell culture supernatant (HGF Human ELISA Kit, Abcam, Cambridge, UK). The absorbance was measured at 450 nm. Data were obtained from seven independent samples, and the data were statistically analyzed.

Western blotting and immunohistochemical staining. Western blotting was performed as described previously.[5] Briefly, 5×10^4 of ALDH1^{high} cells and ALDH1^{low} cells were lysed in 100 μL of SDS sample buffer. Anti-ALDH1 mouse monoclonal antibody (clone: 44/ALDH; BD Biosciences, San Jose, CA, USA) was used at 1000-times dilution. Anti-HGF goat polyclonal antibody (R&D Systems, Minneapolis, MN, USA) and anti-MET goat polyclonal antibody (R&D Systems) were used at 1000-times dilution. Anti-β-Actin mouse monoclonal antibody (Sigma, St. Louis, MO, USA) was used at 2000-times dilution. Anti-mouse IgG + IgM and anti-goat IgG and IgM second antibodies (KPL) were uses at 2000-times dilution. The membrane was visualized with Chemiluminescent HRP Substrate (Millipore, Billerica, MA, USA) according to the manu-

[4]To whom correspondence should be addressed.
E-mails: hirohash@sapmed.ac.jp; torigoe@sapmed.ac.jp

doi: 10.1111/cas.12104

facturer's protocol, and pictures were taken by Odyssey Fc Imaging System (LI-COR, Lincoln, NE, USA).

Immunohistochemical staining using formalin-fixed paraffin-embedded sections of surgically resected prostate carcinoma was performed as described previously.[6] Anti-ALDH1 mouse antibody was used at 250-times dilution. Anti-HGF mouse monoclonal antibody (Abcam) was used at 10 μg/mL. Anti-SOX2 rabbit polyclonal antibody (Invitrogen, Palo Alto, CA, USA) was used at 250-times dilution. Peroxidase-labeled goat anti-rabbit polyclonal antibody (Nichirei, Tokyo, Japan) was used as manufacturer's protocol and visualized by 3,3'-diaminobenzidine tetrachloride (DAB). Alkaline phosphatase-labeled goat anti-mouse polyclonal antibody (Nichirei) was used according to the manufacturer's protocol and visualized by New Fuchsin (Nichirei). Nucleus brown staining was judged as positive staining for SOX2, and cytoplasm red staining was judged as positive staining for ALDH1 and HGF.

Prostasphere formation assay. Isolated ALDH1^{high} and ALDH1^{low} cells were seeded into an Ultra-Low Attachment Surface culture six-well plate (CORNING, Tewksbury, MA, USA) at a concentration of 8×10^3/well and cultured in DMEM/F12 medium (Invitrogen, San Diego, CA, USA) supplemented with 20 ng/mL of epidermal growth factor (EGF; Sigma-Aldrich, St. Louis, MO, USA), 10 ng/mL of basic fibroblast growth factor (bFGF; Sigma-Aldrich), 10 ng/mL of HGF (Sigma-Aldrich) and 10 ng/mL IGF-1 (Sigma-Aldrich). The morphology of the cells was assayed and pictures were taken under a light microscope every day. For inhibition of HGF, anti-HGF antibody was supplemented at a concentration of 20 ng/mL. Anti-HLA class I antibody (clone: W6/32) was used as a negative control. Prostate myofibroblast culture supernatant was obtained from myofibroblasts cultured in serum-free DMEM media for 2 days. The myofibroblast supernatant was supplemented in a sphere culture condition at 50% (v/v).

***MET* mRNA knockdown by siRNA.** A *MET* gene knockdown experiment was performed using small interfering RNA (siRNA). MET siRNA duplex was obtained from Validated Stealth RNAi siRNA systems (Oligo ID; HSS106479; Invitrogen). Negative control siRNA was obtained from Invitrogen. 22Rv1 cells were seeded into a 24-well plate, and transfections were carried out using Lipofectamine RNAi max (Invitrogen) in Opti-MEM according to the manufacturer's instructions.

Analysis of cell growth. Negative control cells and MET knocked-down 22Rv1 cells were each seeded into a six-well plate at 5×10^4 cells per well. After incubation for 24, 48 and 72 h, the cells were removed by trypsin and viable cell numbers were determined using Countess (Life Technologies).

Xenograft transplantation into NOD/SCID mice. Experiments using animals were done in accordance with the institutional guidelines for the use of laboratory animals. Bulk and MET knocked-down cells were re-suspended at concentrations of 1×10^3 cells in 100 μL of PBS and Matrigel (BD Biosciences) mixture (1:1). The cells were injected subcutaneously into the right and left mid-back areas of anesthetized 6-week-old male non-obese diabetic/severe combined immunodeficiency (NOD/SCID) mice. The progression of cancer cell growth was monitored weekly, and mice underwent autopsy at 50 days after cell injection.

Statistical analysis. Data are presented as means ± SD from at least three independent experiments. Statistical analysis of the data was performed by Student's *t*-test. *P*-values of ≤ 0.05 were considered statistically significant.

Results

Preferential growth factor gene expressions in prostate cancer stem cells. We previously reported the successful isolation of prostate CSCs/CICs from the prostate carcinoma cell line 22Rv1 by the ALDEFLUOR assay as ALDH^{high} cells, and we found that more than 200 genes were overexpressed in prostate CSCs/CICs compared with expression levels in non-CSCs/CICs.[3] The overexpressed genes included the growth factors *IGF1* and *HGF*. Activation of c-MET, the receptor for HGF, is related to a stem-like phenotype in prostate cancer cells,[7] and we therefore further analyzed the function of HGF in this study. Upregulation of the expression of *IGF1* and *HGF* was confirmed by RT-PCR analysis, whereas the expression levels of *MET* showed no significant difference in ALDH^{high} and ALDH^{low} cells (Fig. 1A). Hepatocyte growth factor protein expression level was higher in ALDH1^{high} cells than in ALDH1^{low} cells, whereas MET protein expression level were similar in ALDH1^{high} cells and ALDH1^{low} cells (Fig. 1B). Stem cell markers including SOX2, POU5F1 and NANOG were described to be overexpressed in prostate CSCs/CICs.[8] To address expressions of ALDH1 and HGF in stem cells of prostate cancer tissue, we performed double immunohistochemical staining using anti-ALDH1 antibody, anti-HGF antibody and anti-SOX2 antibody as a prostate CSC/CIC marker. Part of SOX2-positive prostate adenocarcinoma cells exhibited positive expression of ALDH1 and HGF (Fig. 1C). Thus ALDH1 and HGF proteins were expressed in prostate CSCs/CICs in primary prostate cancer tissue.

Prostate cancer stem cells secrete a growth factor, HGF. Hepatocyte growth factor protein secretion by ALDH^{high} cells was investigated by ELISA. The mean HGF level in ALDH^{high} cell culture medium was 7.499 pg/mL, whereas HGF level in ALDH^{low} cell culture medium was 1.082 pg/mL (Fig. 1D), and the difference was statistically significant ($P < 0.05$).

Growth factors enhance prostasphere formation. Non-adherent sphere-forming assays are increasingly being used to evaluate stem cell phenotypes in normal tissues as well as putative CSCs/CICs. We previously reported that ALDH1^{high} cells have higher sphere-forming ability than that of ALDH1^{low} cells using EGF and bFGF.[3] In the present study, we found that growth factors (HGF and IGF1) are overexpressed in ALDH1^{high} cells compared with the expression in ALDH1^{low} cells, and we therefore investigated the effects of growth factors on sphere-forming ability of prostate carcinoma cells. Eight thousand prostate carcinoma cells were incubated in ultra-low attachment surface culture dishes in serum-free culture media with or without additional growth factors (IGF1 and HGF). The addition of HGF onto EGF and bFGF enhanced sphere formation, whereas the addition of IGF1 onto EGF and bFGF did not enhance sphere formation. The addition of both HGF and IGF1 resulted in maximum sphere formation of ALDH1^{high} cells (Fig. 2A). Growth factors increased sphere formation of both ALDH1^{high} and ALDH1^{low} cells, and ALDH1^{high} cells cultured with growth factors showed the highest sphere formation efficiency (Fig. 2B,C).

Since ALDH1^{high} cells secrete HGF, we hypothesized that HGF secreted from ALDH1^{high} cells has a role in sphere formation of ALDH1^{high} cells in an autocrine fashion. We therefore added anti-HGF mAb to the sphere culture supplemented with only EGF and bFGF. The anti-HGF mAb significantly suppressed sphere formation of ALDH1^{high} cells (Fig. 3).

Since HGF is secreted from mesenchymal cells, we hypothesized that HGF secreted from stromal cells also has a role in the maintenance of prostate CSCs/CICs. To address this question, myofibroblasts derived from the prostate were cultured, and the culture supernatant was added to ALDH1^{high} cells. The myofibloblast supernatant increased the sphere formation of ALDH1^{high} cells, which was inhibited by anti-HGF mAb (Fig. 4). These results indicate that HGF derived from both ALDH1^{high} cells and stromal cells has a role in the maintenance of prostate CSCs/CICs.

c-MET has a role in the maintenance of prostate cancer stem cells both *in vitro* and *in vivo*. To confirm the roles of HGF in

doi: 10.1111/cas.12104

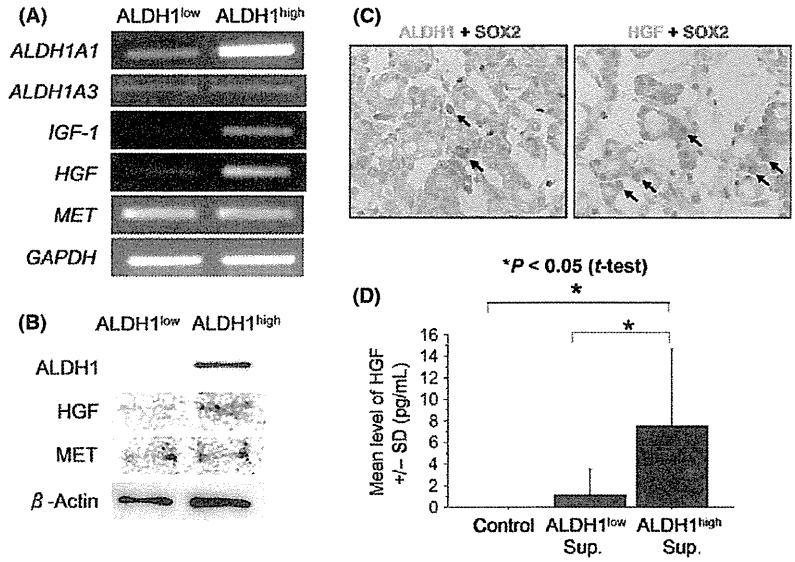

Fig. 1. Expression of growth factors and receptors in prostate cancer stem-like cells (CSCs)/cancer-initiating cells (CICs). (A) Reverse transcription-polymerase chain reaction (RT-PCR) of *HGF*, *IGF1* and *MET* in ALDH1^{high} cells and ALDH1^{low} cells. *HGF*, *IGF1* and *MET* mRNA expression was evaluated by RT-PCR. *Glyceraldehyde 3-phosphate dehydrogenase* (*GAPDH*) was used as a positive control. (B) Western blot analysis of ALDH1, hepatocyte growth factor (HGF) and c-MET. Western blot analysis using 5×10^4 ALDH1^{high} cells and ALDH1^{low} cells was performed. Anti-β-Actin was used as an internal control. (C) ALDH1 and HGF expression in primary prostate CSCs/CICs. Prostate adenocarcinoma tissue was stained by anti-SOX2 and anti-ALDH1 (left panel) and anti-SOX2 and anti-HGF (right panel). Nucleus brown staining was judged as positive staining for SOX2, and cytoplasm red staining was judged as positive staining for ALDH1 and HGF. Arrows indicate SOX2 and ALDH1 double positive cells and SOX2 and HGF double positive cells. Magnification, ×400. (D) Hepatocyte growth factor secretion by ALDH1^{high} cells and ALDH1^{low} cells. Isolated ALDH1^{high} cells and ALDH1^{low} cells were incubated in a 96-well plate for 2 days. Then HGF was evaluated by enzyme linked immunosorbent assay (ELISA). Control represents only culture medium. Asterisks represents statistically significant difference ($P < 0.05$, *t*-test).

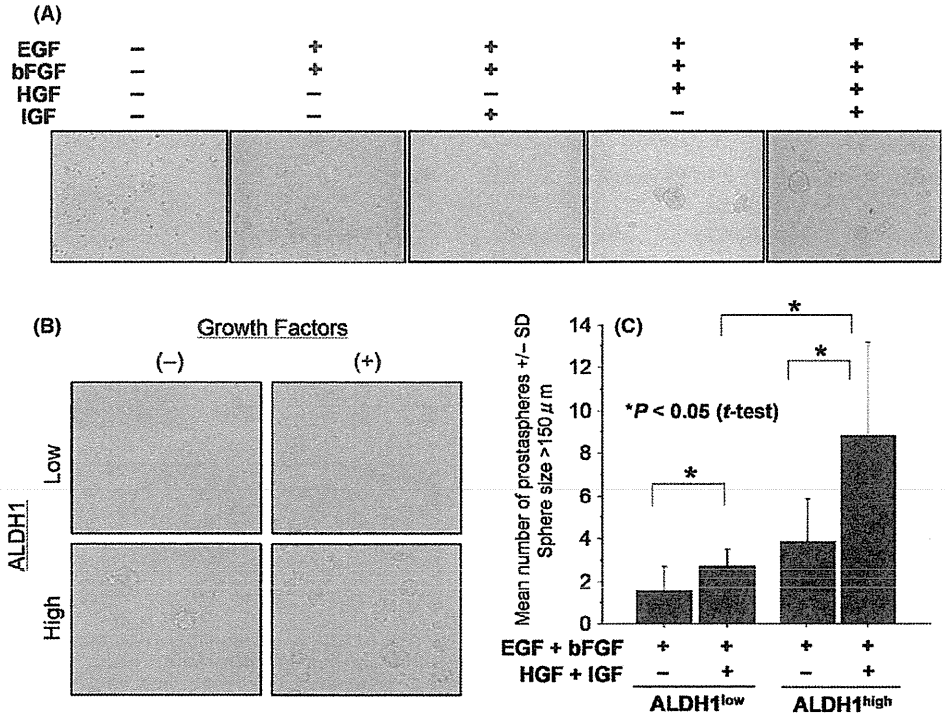

Fig. 2. Growth factors enhance prostasphere formation *in vitro*. (A) Prostasphere formation was increased by hepatocyte growth factor (HGF). Prostasphere formation was performed in serum-free Dulbecco's modified eagle medium (DMEM)/F12 media. Growth factors were added to the prostasphere culture. Representative pictures of prostaspheres are shown. Magnification, ×100. (B) Representative pictures of prostaspheres formed by ALDH1^{high} cells and ALDH1^{low} cells. ALDH1^{high} cells and ALDH1^{low} cells were cultured with or without HGF and IGF1. Representative pictures are shown. Magnification ×100. (C) Prostasphere formation of ALDH1^{high} cells and ALDH1^{low} cells with or without growth factors (HGF and IGF1). ALDH1^{high} cells and ALDH1^{low} cells were cultured in serum-free media with or without HGF and IGF1. The numbers of prostaspheres were evaluated at day 3. Asterisks represents statistically significant difference ($P < 0.05$, *t*-test).

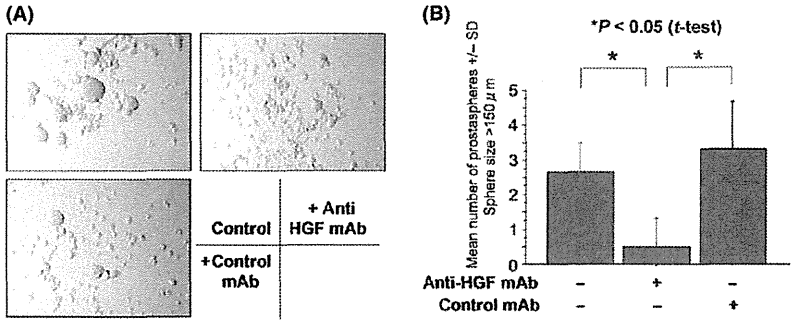

Fig. 3. Prostasphere formation was inhibited by anti-hepatocyte growth factor (HGF) antibody. ALDH1^{high} cells were cultured in Dulbecco's modified eagle medium (DMEM)/F12 medium supplemented with epidermal growth factor (EGF) and basic fibroblast growth factor (bFGF). Anti-HGF antibody and control antibody were added to the culture. Representative pictures are shown (A). Magnification, ×100. The numbers of prostaspheres were evaluated at day 3 (B). Asterisks represents statistically significant difference ($P < 0.05$, *t*-test).

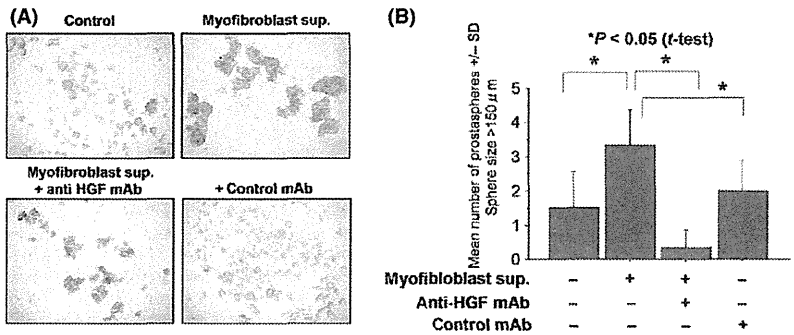

Fig. 4. Prostasphere formation was increased by supernatant of prostate myofibroblasts. ALDH1^{high} cells were cultured in Dulbecco's modified eagle medium (DMEM)/F12 medium supplemented with epidermal growth factor (EGF) and basic fibroblast growth factor (bFGF). Fifty percent (v/v) of myofibroblast culture supernatant was added to culture. Anti-HGF antibody and control antibody were added to the culture. Representative pictures are shown (A). Magnification, ×100. The numbers of prostaspheres were evaluated at day 3 (B). Asterisks represents statistically significant difference ($P < 0.05$, *t*-test).

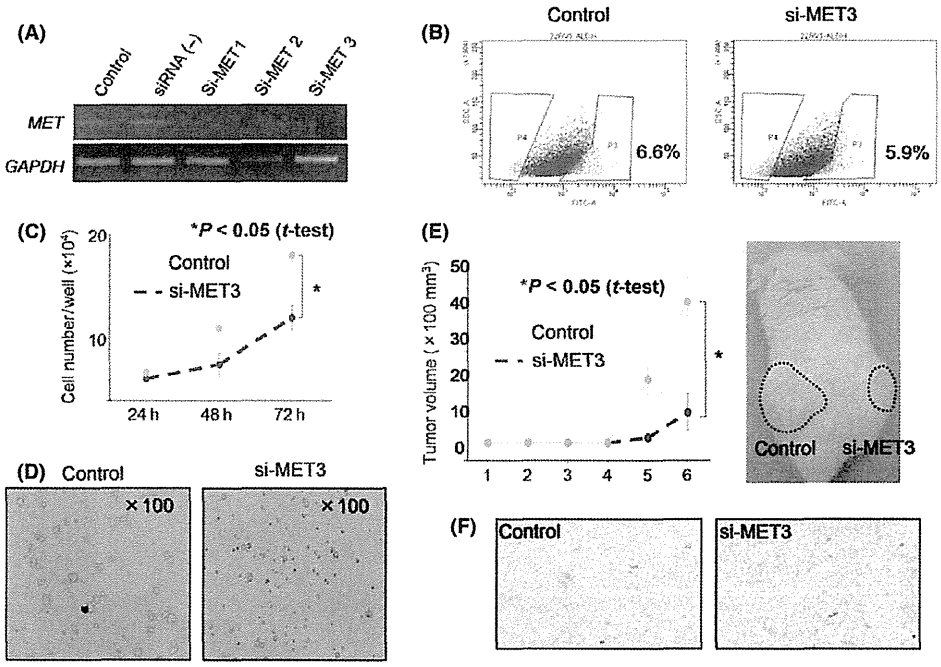

Fig. 5. c-MET has a role in the maintenance of prostate cancer stem-like cells (CSCs)/cancer-initiating cells (CICs). (A) Reverse transcription-polymerase chain reaction (RT-PCR) of MET knockdown cells. MET-specific siRNA and control siRNA were transfected into 22Rv1 cells. Two days after transfection, total RNA was purified and analyzed by RT-PCR. Glyceraldehyde 3-phosphate dehydrogenase (GAPDH) was used as an internal control. (B) ALDEFLUOR assay of MET knockdown cells. MET siRNA3- and control siRNA-transfected 22Rv1 cells were analyzed by ALDEFLUOR assay. Percentages indicate rates of ALDH1^{high} cells. (C) MET gene knockdown inhibited cell growth *in vitro*. MET siRNA3- and control siRNA-transfected 22Rv1 cells were seeded into a six-well plate, and cell numbers were counted at 24, 48 and 72 h. An asterisk represents a statistically significant difference ($P < 0.05$, *t*-test). (D) MET gene knockdown inhibited prostasphere formation *in vitro*. MET siRNA3- and control siRNA-transfected 22Rv1 cells were seeded into an Ultra-Low Attachment plate and cultured for 3 days. (E) MET gene knockdown inhibited tumor initiation *in vivo*. MET siRNA3- and control siRNA-transfected 22Rv1 cells were transplanted into male NOD/SCID mice subcutaneously. Tumor growth was measured every week. Tumor growth curve and a representative picture are shown. An asterisk represents a statistically significant difference ($P < 0.05$, *t*-test). (F) ALDH1 expression in MET knockdown tumor. ALDH1 expression was investigated by immunohistochemical staining. Representative pictures are shown. Magnification, ×100.

doi: 10.1111/cas.12104

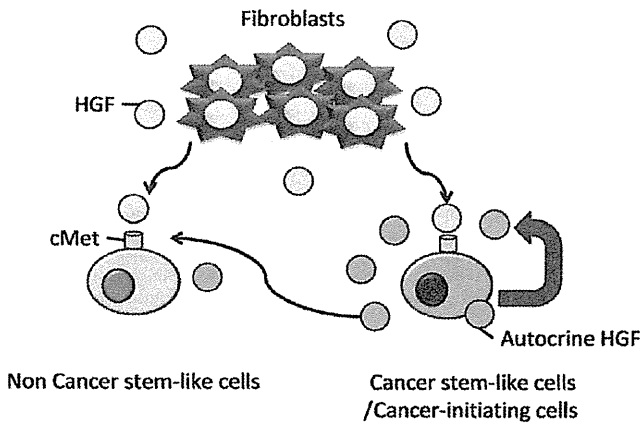

Fig. 6. Model of the maintenance of prostate cancer stem-like cells (CSCs)/cancer-initiating cells (CICs)through hepatocyte growth factor (HGF)/c-MET signaling.

cell growth and tumorigenicity, we performed gene-knockdown studies using siRNA of c-MET, the HGF receptor (Fig. 5A). Gene knockdown of c-MET mRNA did not affect the rate of ALDH1^{high} cells, whereas it suppressed cell growth *in vitro* and sphere formation (Fig. 5B–D).

To evaluate the role of HGF in tumorigenicity, 1×10^3 negative control and siRNA-transfected 22Rv1 cells were injected into the backs of NOD/SCID mice ($n = 4$). The tumors derived from siRNA-transfected 22Rv1 cells were significantly smaller than those derived from negative control cells ($P < 0.05$, Fig. 5E), whereas ALDH1 expression was not suppressed by c-MET siRNA (Fig. 5F). These results indicate that MET signaling has a role in the maintenance of prostate CSCs/CICs, whereas it has no role in the expression of ALDH1.

Discussion

Hepatocyte growth factor is a paracrine factor produced by cells of mesenchymal origin, while the HGF receptor, c-MET, is expressed by epithelial and endothelial cells.[9] Hepatocyte growth factor is a heterodimeric protein comprised of a 55–60-kDa α chain and a 32–34-kDa β chain linked by a single disulfide bond. c-MET is a tyrosine kinase receptor with a single transmembrane spanning region and a conserved tyrosine kinase domain. c-MET is translated as a single polypeptide chain that is proteolytically cleaved to form an approximately 145-kDa β heavy chain and an approximately 35-kDa α light chain linked by a single disulfide bond. Signal transduction by HGF leads to a variety of biological responses including proliferation, migration and morphogenesis. Hepatocyte growth factor plays important roles in the progression of many invasive and metastatic cancers.[10] The interaction between tumor cells and their surrounding stromal environment remains a crucial factor governing tumor invasion and metastasis.

c-MET receptor tyrosine kinase had been shown to be involved in tumor proliferation and progression, and overexpression of c-MET has been shown to be associated with advanced prostate cancer.[11–15] These findings suggested that the strategy of inhibiting the activation of both HGF/c-MET and androgen receptor (AR) signaling pathways should be considered in the treatment of advanced prostate cancer. It has recently been reported that c-MET inhibitors demonstrated anti-proliferative efficacy when combined with androgen ablation therapy for advanced prostate cancer.[16]

It has been reported that c-MET was overexpressed in immature DU145 prostate carcinoma cells and that c-MET signaling has a role in induction of a stem-like cell phenotype.[5] On the other hand, c-MET was expressed in both ALDH1^{high} cells and ALDH1^{low} cells derived from 22Rv1 prostate carcinoma cells at similar levels, whereas its ligand HGF was overexpressed in ALDH1^{high} cells.[3] ALDH1^{high} cells secrete a larger amount of HGF than do ALDH1^{low} cells, and HGF together with IGF1 enhanced the efficiency of sphere formation *in vitro*. Gene knockdown of c-MET inhibited cell growth *in vitro* and abrogated the sphere-forming ability and tumor-initiating ability in NOD/SCID mice. Therefore, our results indicate that activation of c-MET signaling has a role in the maintenance of prostate CSCs/CICs and that c-MET activation might be caused by HGF secretion from prostate CSCs/CICs, not by overexpression of c-MET.

Hepatocyte growth factor/c-MET signaling is related to epithelial-mesenchymal transition (EMT), anoikis and dissemination in gastric carcinoma cells, and high expression levels of HGF and c-MET in gastric carcinoma specimens are related to poor prognosis.[17] In colon carcinoma cells, HGF secreted by stromal fibroblasts is required for nuclear localization of β-catenin, which is essential for maintenance of colon CSCs/CICs.[18] Cancer-associated fibroblasts (CAFs) are a candidate of HGF secretion, and we actually confirmed that the culture supernatant of myofibroblasts derived from the prostate enhanced prostasphere formation. Therefore, we hypothesize that both prostate CSCs/CICs and fibroblasts secrete HGF and that HGF has a role in maintenance of prostate CSCs/CICs in autocrine and paracrine fashions. Hepatocyte growth factor may also enable non-CSCs/CICs to obtain malignant phenotypes including stemness in a paracrine fashion through activating the Wnt/β-catenin signal (Fig. 6).

In summary, HGF/c-MET signaling has a major role in the maintenance of prostate CSCs/CICs. Prostate CSCs/CICs secrete HGF, and HGF may stimulate c-MET expressed on prostate CSCs/CICs in an autocrine fashion. Blocking HGF/c-MET autocrine activation might be a promising approach to target prostate CSCs/CICs.

Acknowledgments

This work was supported by Grants-in-Aid for Scientific Research from the Ministry of Education, Culture, Sports, Science and Technology of Japan (grant Nos. 16209013, 17016061, 15659097 and 24592399) for Practical Application Research from the Japan Science and Technology Agency, and for Cancer Research (15-17 and 19-14) from the Ministry of Health, Labor and Welfare of Japan, Ono Cancer Research Fund (to N. S.) and Takeda Science Foundation (to Y. H.). This work was supported in part by the National Cancer Center Research and Development Fund (23-A-44).

Disclosure Statement

The authors have no conflict of interest.

References

1 Park CY, Tseng D, Weissman IL. Cancer stem cell-directed therapies: recent data from the laboratory and clinic. *Mol Ther* 2009; **17**: 219–30.

2 Hirohashi Y, Torigoe T, Inoda S *et al.* Immune response against tumor antigens expressed on human cancer stem-like cells/tumor-initiating cells. *Immunotherapy* 2010; **2**: 201–11.

3 Nishida S, Hirohashi Y, Torigoe T *et al.* Gene expression profiles of prostate cancer stem cells isolated by ALDH activity assay. *J Urol* 2012; **188**: 294–9.

4 Cecchi F, Rabe DC, Bottaro DP. Targeting the HGF/Met signalling pathway in cancer. *Eur J Cancer* 2010; **46**: 1260–70.
5 Inoda S, Hirohashi Y, Torigoe T *et al.* Cep55/c10orf3, a tumor antigen derived from a centrosome residing protein in breast carcinoma. *J Immunother* 2009; **32**: 474–85.
6 Michifuri Y, Hirohashi Y, Torigoe T *et al.* High expression of ALDH1 and SOX2 diffuse staining pattern of oral squamous cell carcinomas correlates to lymph node metastasis. *Pathol Int* 2012; **62**: 684–9.
7 van Leenders GJ, Sookhlall R, Teubel WJ *et al.* Activation of c-MET induces a stem-like phenotype in human prostate cancer. *PLoS ONE* 2011; **6**: e26753.
8 Gu G, Yuan J, Wills M, Kasper S. Prostate cancer cells with stem cell characteristics reconstitute the original human tumor *in vivo*. *Cancer Res* 2007; **67**: 4807–15.
9 Rubin JS, Bottaro DP, Aaronson SA. Hepatocyte growth factor/scatter factor and its receptor, the c-met proto-oncogene product. *Biochim Biophys Acta* 1993; **1155**: 357–71.
10 Peruzzi B, Bottaro DP. Targeting the c-Met signaling pathway in cancer. *Clin Cancer Res* 2006; **12**: 3657–60.
11 Bottaro DP, Rubin JS, Faletto DL *et al.* Identification of the hepatocyte growth factor receptor as the c-met proto-oncogene product. *Science* 1991; **251**: 802–4.
12 Knudsen BS, Edlund M. Prostate cancer and the met hepatocyte growth factor receptor. *Adv Cancer Res* 2004; **91**: 31–67.
13 Humphrey PA, Zhu X, Zarnegar R *et al.* Hepatocyte growth factor and its receptor (c-MET) in prostatic carcinoma. *Am J Pathol* 1995; **147**: 386–96.
14 Kasai S, Sugimura K, Matsumoto K, Nishi N, Kishimoto T, Nakamura T. Hepatocyte growth factor is a paracrine regulator of rat prostate epithelial growth. *Biochem Biophys Res Commun* 1996; **228**: 646–52.
15 Knudsen BS, Gmyrek GA, Inra J *et al.* High expression of the Met receptor in prostate cancer metastasis to bone. *Urology* 2002; **60**: 1113–7.
16 Tu WH, Zhu C, Clark C, Christensen JG, Sun Z. Efficacy of c-Met inhibitor for advanced prostate cancer. *BMC Cancer* 2010; **10**: 556.
17 Toiyama Y, Yasuda H, Saigusa S *et al.* Co-expression of hepatocyte growth factor and c-Met predicts peritoneal dissemination established by autocrine hepatocyte growth factor/c-Met signaling in gastric cancer. *Int J Cancer* 2011; **130**: 2912–21.
18 Vermeulen L, De Sousa E, Melo F, van der Heijden M *et al.* Wnt activity defines colon cancer stem cells and is regulated by the microenvironment. *Nat Cell Biol* 2010; **12**: 468–76.

doi: 10.1111/cas.12104

TISSUE ANTIGENS
IMMUNE RESPONSE GENETICS

Tissue Antigens ISSN 0001-2815

Preferential expression of cancer/testis genes in cancer stem-like cells: proposal of a novel sub-category, cancer/testis/stem gene

R. Yamada[1], A. Takahashi[1], T. Torigoe[1], R. Morita[1], Y. Tamura[1], T. Tsukahara[1], T. Kanaseki[1], T. Kubo[1], K. Watarai[1], T. Kondo[2], Y. Hirohashi[1] & N. Sato[1]

1 Department of Pathology, Sapporo Medical University School of Medicine, Sapporo, Japan
2 Department of Stem Cell Biology, Hokkaido University Graduate School of Medicine, Sapporo, Japan

Key words
cancer stem cell; cancer/testis gene; cancer/testis/stem gene

Correspondence
T. Torigoe
Department of Pathology
Sapporo Medical University School of Medicine
South-1 West-17, Chuo-ku
Sapporo 060-8556
Japan
Tel: +81 11 611 2111
Fax: +81 11 643 2310
e-mail: torigoe@sapmed.ac.jp
and
Y. Hirohashi
Department of Pathology
Sapporo Medical University School of Medicine
South-1 West-17, Chuo-ku
Sapporo 060-8556
Japan
Tel: +81 11 611 2111
Fax: +81 11 643 2310
e-mail: hirohash@sapmed.ac.jp

Received 16 October 2012; revised 13 February 2013; accepted 12 March 2013

doi: 10.1111/tan.12113

Abstract

Cancer/testis (CT) antigens encoded by CT genes are immunogenic antigens, and the expression of CT gene is strictly restricted to only the testis among mature organs. Therefore, CT antigens are promising candidates for cancer immunotherapy. In a previous study, we identified a novel CT antigen, DNAJB8. DNAJB8 was found to be preferentially expressed in cancer stem-like cells (CSCs)/cancer-initiating cells (CICs), and it is thus a novel CSC antigen. In this study, we hypothesized that CT genes are preferentially expressed in CSCs/CICs rather than in non-CSCs/-CICs and we examined the expression of CT genes in CSCs/CICs. The expression of 74 CT genes was evaluated in side population (SP) cells (=CSC) and main population (MP) cells (=non-CSC) derived from LHK2 lung adenocarcinoma cells, SW480 colon adenocarcinoma cells and MCF7 breast adenocarcinoma cells by RT-PCR and real-time PCR. Eighteen genes (*MAGEA2, MAGEA3, MAGEA4, MAGEA6, MAGEA12, MAGEB2, GAGE1, GAGE8, SPANXA1, SPANXB1, SPANXC, XAGE2, SPA17, BORIS, PLU-1, SGY-1, TEX15* and *CT45A1*) showed higher expression levels in SP cells than in MP cells, whereas 10 genes (BAGE1, BAGE2, BAGE4, BAGE5, XAGE1, LIP1, D40, HCA661, TDRD1 and TPTE) showed similar expression levels in SP cells and MP cells. Thus, considerable numbers of CT genes showed preferential expression in CSCs/CICs. We therefore propose a novel sub-category of CT genes in this report: cancer/testis/stem (CTS) genes.

Introduction

Cancer treatment has been improved to some degree in the past several decades. However, cancer is still a biologically malignant disease that may result in death. It is expected that cancer immunotherapy will become an effective approach to treat cancer. Various tumor-associated antigens (TAAs) have been identified in the past several decades, and cancer immunotherapy targeting TAAs has become a reality (1, 2). TAAs can be classified into several categories according to their expression in cancer cells and normal cells (3). One of the major categories is cancer/testis (CT) genes, which are expressed in cancer cells and only in the testis among human matured organs (4). The testis does not express the major histocompatibility complex molecule, and CT antigens are not expressed on the surface of cells as antigenic peptides. The testis is therefore not accessible by cytotoxic T lymphocytes (CTLs), and the testis is thus called an 'immunological privileged' organ. Some proteins coded by CT genes are immunogenic to the cellular immune system and humoral immune system, and proteins coded by CT genes are therefore considered to be promising targets for cancer immunotherapy (4).

Cancer stem-like cells (CSCs)/cancer-initiating cells (CICs) are defined as a small population of cancer cells that have (i) high tumor-initiating ability, (ii) self-renewal ability and (iii) differentiation ability (5). CSCs/CICs are resistant to

chemotherapy and radiotherapy and are therefore considered to be responsible for cancer recurrence and distant metastasis (6). As previous studies have shown that CSCs/CICs are sensitive to immune systems, cancer immunotherapy targeting them is a possible and promising approach (7–10). To achieve a CSC/CIC-specific immune reaction, it is essential to identify TAAs that are expressed in CSCs/CICs.

In our previous study, we identified a novel CT antigen, DNAJB8 (11). DNAJB8 has a role in the maintenance of CSCs/CICs and is expressed preferentially in CSCs/CICs than in non-CSCs/non-CICs. DNAJB8 is therefore a novel CSC antigen. Thus, DNAJB8 is a CT antigen and also a cancer stem antigen. In this study, we analyzed the expression profiles of known CT genes in CSCs/CICs and non-CSCs/non-CICs. Therefore we propose a novel sub-category of CT genes called the cancer/testis/stem (CTS) that are expressed in the testis and CSCs.

Materials and methods

Cell lines and isolation of side and main population cells

The LHK2 lung adenocarcinoma cell line was found by Hirohashi et al. (12). SW480 colon adenocarcinoma cells and MCF7 breast adenocarcinoma cells were purchased from ATCC. LHK2, SW480 and MCF7 cells were cultured in DMEM (Sigma-Aldrich, St. Louis, MO) supplemented with 10% FBS (Life Technologies, Grand Island, NY).

Side population (SP) cells were isolated as described previously using Hoechst 33342 dye (Lonza, Basel, Switzerland) with some modifications (13). Briefly, cells were resuspended at 1×10^6/ml in pre-warmed DMEM supplemented with 5% FBS. Hoechst 33342 dye was added at a final concentration of 2.5 μg/ml in the presence or absence of verapamil (50 μM; Sigma-Aldrich) and the cells were incubated at 37°C for 90 min with intermittent shaking. Analyses and sorting were performed with a FACSAria II cell sorter (BD Biosciences, San Jose, CA).

RT-PCR analysis

Reverse transcription-polymerase chain reaction (RT-PCR) analysis was performed as described previously (14). Human Multiple Tissue cDNA Panel II (Takara Bio, Otsu, Japan) was used as templates of normal adult testis tissue cDNA. PCR amplification was performed in 20 μl of PCR mixture containing 0.2 μl of the cDNA mixture, 0.5 μl of Taq DNA polymerase (QIAGEN, Duesseldorf, Germany) and 12 pmol of primers. The PCR mixture was initially incubated at 94°C for 2 min, followed by 35 cycles of denaturation at 94°C for 15 s, annealing at 60°C for 30 s and extension at 68°C for 30 s. The PCR products were visualized with ethidium bromide staining under UV light after electrophoresis on 1.2% agarose gel. Primers used in experiments are summarized in the supplemental Table S1. Human testis cDNA was used as a positive control and water was used as a negative control.

Quantitative PCR (qPCR)

Quantitative real-time PCR was performed using an ABI PRISM 7000 sequence detection system (Life Technologies) according to the manufacturer's protocol. Primers and probes were designed by the manufacturer (TaqMan gene expression assays; Life Technologies). Thermal cycling was performed using 40 cycles of denaturation at 95°C for 15 s followed by annealing at 60°C for 1 min. Each experiment was performed triplicate, with normalization to the *GAPDH* gene as an internal control.

Statistical analysis

Statistical analysis between two groups of real-time PCR was performed by Student's *t* test and that between two groups of X-CT genes was performed by the chi-squared test.

Results

Preferential expression of some CT genes in CSCs/CICs

SP cells derived from lung adenocarcinoma cells, LHK2, colon adenocarcinoma cells, SW480, and breast adenocarcinoma cells, MCF7, are enriched with CSCs/CICs, and we therefore used it as a source of CSCs/CICs and MP cells as a source of non-CSCs/non-CICs (9, 13, 15). SP cells and MP cells were isolated from LHK2 lung adenocarcinoma cells, SW480 colon adenocarcinoma cells and MCF7 breast adenocarcinoma cells. To evaluate the expression of known CT genes in CSCs/CICs, RT-PCR was performed using SP and MP cells. A total of 74 CT genes were evaluated (Figure 1).

MAGEA2, MAGEA3, MAGEA6 and *GAGE8* were preferentially expressed in SP cells derived from LHK2 and SW480 cells, whereas *MAGEA2*, *MAGEA3*, *MAGEA6* and *GAGE8* were not detectable in both SP and MP cells derived from MCF7 cells. *MAGEA4*, *MAGEB2*, *GAGE1, SPANXA1, SPANXB1, SPANXC* and *BORIS* were preferentially expressed in SP cells derived from SW480 cells, whereas *MAGEA4, MAGEB2, GAGE1, SPANXA1, SPANXB1, SPANXC* and *BORIS* were not detectable in both SP and MP cells derived from LHK2 cells and MCF7 cells. *XAGE2, SGY-1* and *CT45A1* were preferentially expressed in SP cells derived from LHK2 cells, whereas *XAGE2, SGY-1* and *CT45A1* were not detectable in SP and MP cells derived from SW480 and MCF7 cells. *MAGEA12* was preferentially expressed in SP cells derived from LHK2 and SW480 cells, whereas *MAGEA12* was expressed in both SP and MP cells derived from MCF7 cells at similar levels. *SPA17*, *PLU-1* and *TEX15* were preferentially expressed in SP cells derived from LHK2 cells, whereas *SPA17*, *PLU-1* and *TEX15* were expressed in both SP and MP cells derived from SW480

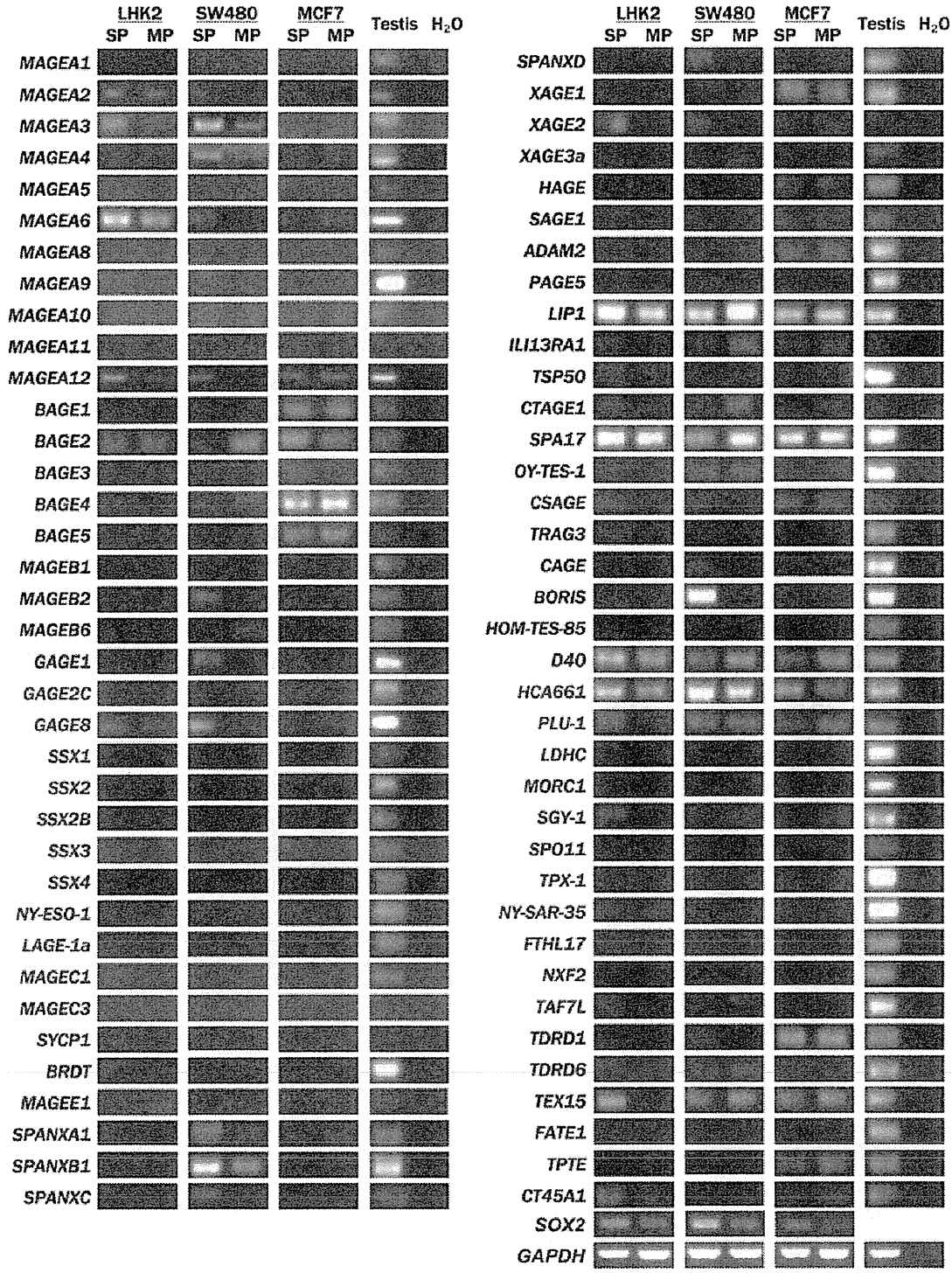

Figure 1 Expression of cancer/testis (CT) genes in cancer stem-like cell (CSCs)/cancer-initiating cell (CICs) and non-CSCs/CICs. The expression of CT genes in CSCs/CICs and non-CSCs/CICs was evaluated by RT-PCR. Side population (SP) cells were used as CSCs/CICs, and main population (MP) cells were used as non-CSCs/CICs. *SOX2* was used as a stem cell marker. Testis cDNA was used as a positive control and water was used as a negative control. *GAPDH* was included as a control for DNA quality.

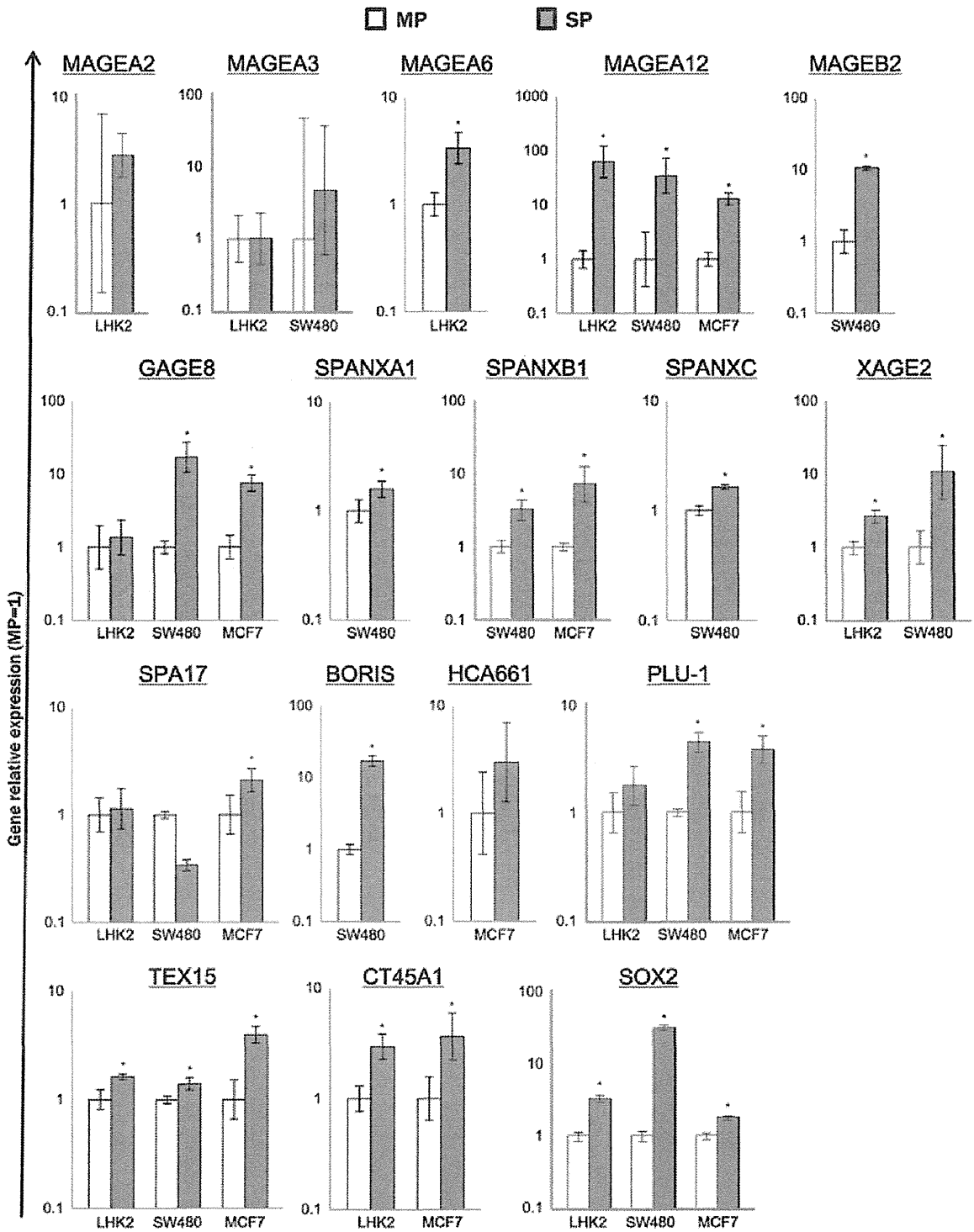

Figure 2 Real-time PCR of cancer/testis (CT) genes in cancer stem-like cell (CSCs)/cancer-initiating cell (CICs). The expression of CT genes in CSCs/CICs and non-CSCs/CICs was evaluated by real-time PCR. *SOX2* was used as a stem cell marker. Data represent means ± SD. Asterisks represent significant differences (*t*-test, $P < 0.05$).

and MCF7 at similar levels. Therefore, *MAGEA2, MAGEA3, MAGEA4, MAGEA6, MAGEA12, MAGEB2, GAGE1, GAGE8, SPANXA1, SPANXB1, SPANXC, BORIS, XAGE2, SPA17, PLU-1, SGY-1, TEX15* and *CT45A1* were preferentially expressed in SP cells. On the other hand, *BAGE1, BAGE2, BAGE4, BAGE5, XAGE1, LIP1, D40, HCA661, TDRD1* and *TPTE* were expressed in both SP cells and MP cells at similar levels. The expression of *MAGEA1, MAGEA5, MAGEA8, MAGEA9, MAGEA10, MAGEA11, BAGE3, MAGEB1, MAGEB6, GAGE2C, SSX1, SSX2, SSX2B, SSX3, SSX4, NY-ESO-1, MAGEC1, MAGEC3, SYCP1, BRDT1, MAGEE1, XAGE3a, HAGE, SAGE1, ADAM2, PAGE5, IL13RA1, TSP50, CTAGE1, OY-TES-1, CSAGE, TRAG3, CAGE, HOM-TES-85, LDHC, MORC1, SPO11, TPX-1, NY-SAR-35, FTHL17, TDRD6* and *FATE1* was undetectable or very weak in SP and MP cells derived from LHK2, SW480 and MCF7 cells.

The data by RT-PCR were confirmed by quantitative PCR (qPCR) (Figure 2). The expression levels of *MAGEA2, MAGEA3, MAGEA4, MAGEA6, MAGEA12, MAGEB2, GAGE1* and *GAGE8* were higher than those of MP cells by RT-PCR and so we analyzed the data by qPCR. The expression levels of *MAGEA6*, *MAGEA12*, *MAGEB2* and *GAGE8* in SP cells were significantly higher than that of MP cells, while the expressions of *MAGEA2* and *MAGEA3* were higher than that of MP cells, but the difference was not significant. *MAGEA4* and *GAGE1* were detectable in SP cells derived from SW480 cells, but they were not detectable in MP cells derived from SW480; thus we could not compare those expression levels. The expression levels of *SPANXA1*, *SPANXB1* and *SPANXC* in SP cells derived from SW480 cells were higher than those of MP cells by qPCR. *SPANXB2* mRNA was detectable also in MCF7 cells, and the expression level of *SPANXB1* in SP cells was higher than that of MP cells. The expression profiles of *XAGE2*, *BORIS*, *HCA661*, *PLU-1*, *TEX15* and *CT45A1* were confirmed by qPCR. The expression of *SGY-1* in LHK2 SP cells was higher than that of LHK2 MP cells, while we could not detect mRNA by qPCR. The expression of *SPA17* in LHK2 SP cells was same as LHK2 MP cells, and *SPA17* in SW480 SP cells was lower than that of SW480 MP cells and *SPA17* in MCF7 SP cells was higher than that of MCF7 MP cells.

As many CT genes showed preferential expression in SP cells rather than in MP cells, we propose a sub-category of CT genes: CTS genes that are expressed in the testis and CSCs (Figure 3). More than half of the CT genes are encoded by a gene located on X chromosome (X-CT genes). Twelve of the 18 CTS genes (67%) are located on the X chromosome, whereas only 2 of the 10 shared antigens (20%) are located on the X chromosome, and the difference is statistically significant ($P = 0.038$; Table 1).

Discussion

CT genes are expressed in several stages of spermatogenesis including spermatogonial stem cells, spermatogonium, spermatocytes, spermatids and spermatozoa (16). In some cases, CT genes are also expressed in the placenta and ovary. CT genes have a role in spermatogenesis, and some of them have been reported to have role in tumorigenesis. However, roles of most CT genes in cancer cells are still elusive (16). The expression of CT genes is controlled by epigenetic mechanisms of demethylation of promoter regions (17). More than half of the CT genes are located on the X chromosome. Sixty-seven percentage of CTS genes are located on the X chromosome, whereas only 20% of the shared CT genes are located on the X chromosome. The biological meaning of this difference is still elusive. X-CT genes are preferentially expressed in a more immature state of spermatogenesis (spermatogonial stem cells), whereas non-X-CT genes are preferentially expressed in more matured stages of spermatogenesis. We therefore hypothesize that the roles of X-CT genes in spermatogonial stem cells are also important in maintenance of CSCs/CICs.

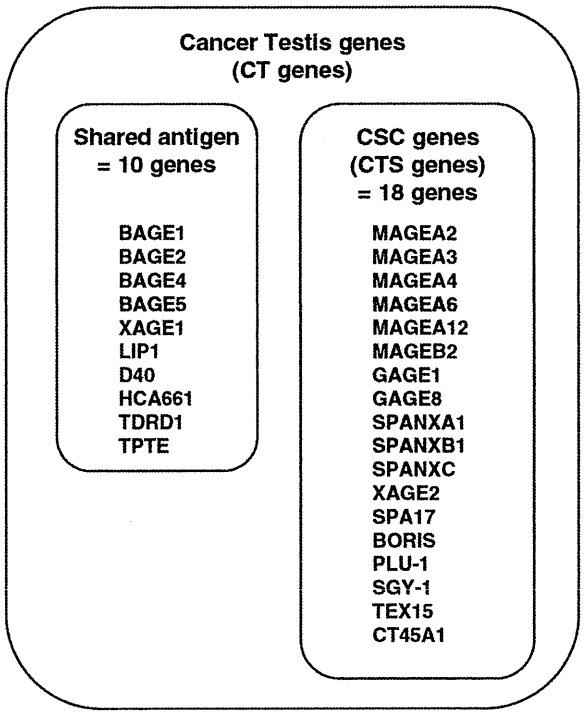

Figure 3 Categorization of cancer/testis (CT) genes.

Antigens coded by CT genes are expressed in a variety of malignant diseases, and humoral and cellular immune responses to the proteins coded by CT genes have been observed in patients with malignant disease (4, 18, 19). Thus, CT genes are considered to be ideal and promising targets for cancer immunotherapy. Indeed, MAGEA2, MAGEA3, MAGEA4, MAGEA6, MAGEA12 and GAGE1 have been shown to be recognized by CTLs (20, 21). On the other hand, MAGEB2, GAGE8, SPANXA1, SPANXB1, SPANXC,

Table 1 Summary of cancer/testis genes

CT genes	Alias	Chromosomes[a]
Summary of CTS genes		
MAGEA2	CT1.2	Xq28
MAGEA3	CT1.3	Xq28
MAGEA4	CT1.4	Xq28
MAGEA6	CT1.6	Xq28
MAGEA12	CT1.12	Xq28
GAGE1	CT4.1	Xp11.23
GAGE8	CT4.8	Xp11
SPANXA1	CT11.1	Xq27.2
SPANXB1	CT11.2	Xq27.1
SPANXC	CT11.3, CTp11	Xq27.2
XAGE2	CT12.2	Xp11.22-p11.21
SPA17	CT22, SP17	11q24.2
CTCFL	CT27, BORIS	20Q13.31
KDM5B	CT31, PLU-1	1q32.1
DKKL1	CT34, SGY-1	19q13.3
TEX15	CT42	8p22
CT45A1	CT45.1	Xq26.1
Summary of shared genes		
BAGE	CT2.1, BAGE1	21p11.1
BAGE2	CT2.2	21p
BAGE4	CT2.4	21p11.1
BAGE5	CT2.5	13cen
XAGE1A	CT12.1a, XAGE1	Xp11.22
CASC5	CT29, D40	15q14
TFDP3	CT30, HCA661	Xq26.2
TDRD1	CT41.1	10p26.11
TPTE	CT44	21p11.1
CENPJ	LIP1, LAP, CPAP	13q12.12

CTS, cancer/testis/stem genes.
[a]The difference in frequencies of X-CT genes (localization in the X chromosome) was analyzed by the chi-squared test. $P = 0.038$.

XAGE2, SPA17, BORIS, PLU-1, SGY-1 TEX15 and CT45A1 have not been reported to be recognized by CTLs yet. In this study, we found that MAGEA12 and TEX15 are expressed in LHK2 lung carcinoma, SW480 colon carcinoma and MCF7 breast carcinoma CSCs/CICs; while the other genes exhibited different expression pattern. MAGEA4, MAGEA6, MAGEB2, SPANXA1, SPANXC and BORIS were preferentially expressed in SP cells derived from SW480 cells, but not expressed in LHK2 and MCF7 cells. These expression profiles indicate that MAGEA12 and TEX15 might be antigens that are expressed in several types of CSCs/CICs, while other antigens are expressed in CSCs/CICs derived from restricted organs. There are several potential CTL target peptides carrying HLA-binding anchor motif in amino acid sequences of these gene products (data not shown). Therefore, antigenic peptides derived from CTS antigens are promising targets for CSC/CIC-targeting immunotherapy, and the expression profile of this study will provide significant information.

In our recent review article, we classified TAAs into three groups according to the expression profiles in CSCs/CICs and non-CSCs/non-CICs: (i) CSC antigens, expressed preferentially in CSCs/CICs, (ii) shared antigens, expressed in both CSCs/CICs and non-CSCs/non-CICs and (iii) non-CSC antigens, expressed preferentially in non-CSCs/non-CICs (22). In subsequent works, we found that shared antigens are more potent than non-CSC antigens and that CSC antigens are more potent than shared antigens (11, 23). We therefore hypothesize that expression in only CSCs is important to achieve an efficient anti-tumor effect. Therefore, CTS genes might be promising targets among CT genes, and further analysis of CTS genes especially on immunogenicity to CTLs is expected.

In summary, we showed the preferential expression of CT genes in CSCs/CICs. We therefore propose a novel subcategory of CT genes: CTS genes. CTS genes might be promising targets for cancer immunotherapy.

Acknowledgments

This work was supported by Grants-in-Aid for Scientific Research from the Ministry of Education, Culture, Sports, Science and Technology of Japan (Grant Nos. 16209013, 17016061 and 15659097), for Practical Application Research from the Japan Science and Technology Agency, and for Cancer Research (15-17 and 19-14) from the Ministry of Health, Labor and Welfare of Japan, Ono Cancer Research Fund (to NS) and Takeda Science Foundation (to YH). This work was supported in part by the National Cancer Center Research and Development Fund (23-A-44).

Conflict of interest

The authors have declared no conflicting interests.

References

1. van der Bruggen P, Traversari C, Chomez P et al. A gene encoding an antigen recognized by cytolytic T lymphocytes on a human melanoma. *Science* 1991: **254**: 1643–7.
2. Hirohashi Y, Torigoe T, Inoda S et al. The functioning antigens: beyond just as the immunological targets. *Cancer Sci* 2009: **100**: 798–806.
3. Boon T, Coulie PG, Van den Eynde B. Tumor antigens recognized by T cells. *Immunol Today* 1997: **18**: 267–8.
4. Scanlan MJ, Simpson AJ, Old LJ. The cancer/testis genes: review, standardization, and commentary. *Cancer Immunol* 2004: **4**: 1.
5. Clarke MF, Dick JE, Dirks PB et al. Cancer stem cells – perspectives on current status and future directions: AACR Workshop on cancer stem cells. *Cancer Res* 2006: **66**: 9339–44.
6. Dean M, Fojo T, Bates S. Tumour stem cells and drug resistance. *Nat Rev Cancer* 2005: **5**: 275–84.
7. Todaro M, D'Asaro M, Caccamo N et al. Efficient killing of human colon cancer stem cells by gammadelta T lymphocytes. *J Immunol* 2009: **182**: 7287–96.

8. Castriconi R, Daga A, Dondero A et al. NK cells recognize and kill human glioblastoma cells with stem cell-like properties. *J Immunol* 2009: **182**: 3530–9.
9. Inoda S, Hirohashi Y, Torigoe T et al. Cytotoxic T lymphocytes efficiently recognize human colon cancer stem-like cells. *Am J Pathol* 2011: **178**: 1805–13.
10. Hirohashi Y, Torigoe T, Inoda S et al. Immune response against tumor antigens expressed on human cancer stem-like cells/tumor-initiating cells. *Immunotherapy* 2010: **2**: 201–11.
11. Nishizawa S, Hirohashi Y, Torigoe T et al. HSP DNAJB8 controls tumor-initiating ability in renal cancer stem-like cells. *Cancer Res* 2012: **72**: 2844–54.
12. Hirohashi Y, Torigoe T, Hirai I et al. Establishment of shared antigen reactive cytotoxic T lymphocyte using co-stimulatory molecule introduced autologous cancer cells. *Exp Mol Pathol* 2010: **88**: 128–32.
13. Nakatsugawa M, Takahashi A, Hirohashi Y et al. SOX2 is overexpressed in stem-like cells of human lung adenocarcinoma and augments the tumorigenicity. *Lab Invest* 2011: **91**: 1796–804.
14. Nakatsugawa M, Hirohashi Y, Torigoe T et al. Novel spliced form of a lens protein as a novel lung cancer antigen, Lengsin splicing variant 4. *Cancer Sci* 2009: **100**: 1485–93.
15. Engelmann K, Shen H, Finn OJ. MCF7 side population cells with characteristics of cancer stem/progenitor cells express the tumor antigen MUC1. *Cancer Res* 2008: **68**: 2419–26.
16. Cheng YH, Wong EW, Cheng CY. Cancer/testis (CT) antigens, carcinogenesis and spermatogenesis. *Spermatogenesis* 2011: **1**: 209–20.
17. Fratta E, Coral S, Covre A et al. The biology of cancer testis antigens: putative function, regulation and therapeutic potential. *Mol Oncol* 2011: **5**: 164–82.
18. Sang M, Lian Y, Zhou X, Shan B. MAGE-A family: attractive targets for cancer immunotherapy. *Vaccine* 2011: **29**: 8496–500.
19. Nishikawa H, Maeda Y, Ishida T et al. Cancer/testis antigens are novel targets of immunotherapy for adult T-cell leukemia/lymphoma. *Blood* 2012: **119**: 3097–104.
20. Graff-Dubois S, Faure O, Gross DA et al. Generation of CTL recognizing an HLA-A*0201-restricted epitope shared by MAGE-A1, -A2, -A3, -A4, -A6, -A10, and -A12 tumor antigens: implication in a broad-spectrum tumor immunotherapy. *J Immunol* 2002: **169**: 575–80.
21. Van den Eynde B, Peeters O, De Backer O, Gaugler B, Lucas S, Boon T. A new family of genes coding for an antigen recognized by autologous cytolytic T lymphocytes on a human melanoma. *J Exp Med* 1995: **182**: 689–98.
22. Hirohashi Y, Torigoe T, Inoda S, Morita R, Kochin V, Sato N. Cytotoxic T lymphocytes: sniping cancer stem cells. *Oncoimmunology* 2012: **1**: 123–5.
23. Mori T, Nishizawa S, Hirohashi Y et al. Efficiency of G2/M-related tumor-associated antigen-targeting cancer immunotherapy depends on antigen expression in the cancer stem-like population. *Exp Mol Pathol* 2012: **92**: 27–32.

Supporting Information

The following supporting information is available for this article:

Table S1: List of primers.

Resveratrol inhibits fibrogenesis and induces apoptosis in keloid fibroblasts

Kanae Ikeda, MD, PhD[1]; Toshihiko Torigoe, MD, PhD[2]; Yoshitaka Matsumoto, MD, PhD[1]; Tatsuya Fujita, MD, PhD[1]; Noriyuki Sato, MD, PhD[2]; Takatoshi Yotsuyanagi, MD, PhD[1]

1. Department of Plastic and Reconstructive Surgery, and
2. Department of Pathology, Sapporo Medical University School of Medicine, Sapporo, Japan

Reprint requests:
Dr. K. Ikeda, Department of Plastic and Reconstructive Surgery, Sapporo Medical University School of Medicine, South 1 West 16, Chuo-ku, Sapporo 060-8543, Japan.
Tel: +81 11 611 2111;
Fax: +81 11 615 0916;
Email: peugeot206ccred@yahoo.co.jp

Manuscript received: August 4, 2011
Accepted in final form: March 18, 2013

DOI:10.1111/wrr.12062

ABSTRACT

Keloids are benign dermal fibrotic tumors arising during the wound healing process. The mechanisms of keloid formation and development still remain unknown, and no effective treatment is available. Resveratrol, a dietary compound, has anticancer properties and, from recent studies, it has been suggested that resveratrol may have an antifibrogenic effect on organs such as the liver and kidney. Based on this idea, we investigated its effect on the regulation of extracellular matrix expression, proliferation, and apoptosis of keloid fibroblasts. Type I collagen, α-smooth muscle actin, and heat shock protein 47 expression decreased in resveratrol-treated keloid fibroblasts in a dose-dependent manner. In addition, resveratrol diminished transforming growth factor-β1 production by keloid fibroblasts. We also demonstrated that it suppressed their proliferation and induced apoptosis of the fibroblasts. Conversely, resveratrol did not decrease type I collagen, α-smooth muscle actin, and heat shock protein 47 mRNA expression in normal skin fibroblasts and barely suppressed cell proliferation. Our data indicate that resveratrol may have an antifibrogenic effect on keloid fibroblasts without any adversely effects on normal skin fibroblasts, suggesting the potential application of resveratrol for the treatment of keloids.

Keloid formation is a dermal fibrotic condition characterized by excessive accumulation of mainly type I collagen in the extracellular matrix of the dermis and fibroblast proliferation arising during the wound healing process.[1] Clinically, keloids appear as raised, red, inflexible hard and ugly scar tissue that is itchy and painful. They proliferate beyond the boundaries of the original wound, whereas hypertrophic scars remain within the confines of the original scar border, do not regress spontaneously, and tend to recur after excision.[2] The common treatments for keloids are intralesional corticosteroid injections and intramarginal excision combined with radiation therapy, used individually or in combination with other methods. In the last years, high-dose-rate interstitial brachytherapy has been described that it is effective and safe for preventing recurrence of keloids.[3,4] However, it is not yet widespread in Japan. The basic mechanism involved in keloid development is still unknown and most treatments fail, with a high rate of recurrence after treatment.

A number of studies over the past decade have investigated the etiology of keloids from various angles. The fact that darker skinned individuals are more susceptible to keloid formation indicates a genetic contribution to keloids.[5,6] Other factors that promote the development of keloids are some forms of skin trauma, wound tension, infection, foreign body reactions, and endocrine factors.[7] It is also suggested that keloids have biological differences, including proliferation and apoptosis, between peripheral and central keloid areas, and cultured fibroblasts obtained from keloid lesions lose certain keloid-specific characteristics during cell culture.[8,9] Although the characteristics of keloids are generally known, the mechanisms of keloid formation are not yet clear. The elucidation of pathogenesis of keloids and the development of therapy have been impeded by the absence of a relevant experimental animal model, because keloids are known to occur only in human beings and are not observed in animals.[10]

Other fibroproliferative diseases, including liver cirrhosis, pulmonary fibrosis, cardiovascular disease, progressive kidney disease, and systemic sclerosis, threaten human health. Nevertheless, there are currently no effective treatments. To find an effective therapy for keloids, we examined resveratrol (3,5,4′-trans-trihydroxystilbene), a natural phytoalexin present in grapes, peanuts, and red wine and also identified as an active ingredient of medicinal plants such as the Kojo-kon in Japanese. Resveratrol is a small molecule inducer of the activity of SIRT1 (sitruin, a silent mating type information regulation 2 homolog 1) activity[11] and a widely investigated tumor-preventive agent. The bioactivities of resveratrol have been widely investigated, and many studies have shown that it has therapeutic potential in some diseases, including ischemic heart disease, arteriosclerosis, and cancer.[12,13] Godichaud et al. have described that resveratrol exhibits strong inhibitory effects on cell proliferation, collagen production, expression of α-smooth muscle actin (α-SMA), and secretion of matrix metalloproteinase 2 of liver fibroblasts.[14] On the basis of these results, they concluded that resveratrol could deactivate human liver myofibroblasts. Moreover, in the CCl4 model of liver cirrhosis in rats, it has been indicated that resveratol possesses a strong antifibrogenic effect by inhibiting nuclear factor-kappa B (NF-kB) activity and production of transforming growth factor-β1 (TGF-β1).[15] Thus, resveratrol is

Table 1. The profile of each sample for primary culture

Patient	Sex	Age (years)	Site	Tissue	Treatment
1	Female	31	Pubic region	Keloid	None
2	Female	48	Shoulder	Keloid	None
3		32	Chest	Keloid	None
4	Male	18	Shoulder	Keloid	None
5	Male	48	Chest	Keloid	None
6	Female	25	Ear	Normal skin	None

expected to be a therapeutically effective material for fibrotic diseases, including keloids. To examine whether resveratrol was applicable for the treatment of keloids, a dermal fibrotic condition, we investigated the effects of resveratrol on the proliferation and apoptosis of fibroblasts derived from keloids.

MATERIALS AND METHODS

Media and chemicals

Dulbecco's modified Eagle's medium (DMEM) and fetal bovine serum (FBS) were purchased from Invitrogen (Tokyo, Japan). Ethylenediaminetetraacetic acid (EDTA, 0.02%) was purchased from Boehringer Mannheim (Indianapolis, IN). Resveratrol was purchased from Cayman Chemical Company (Ann Arbor, MI).

Cell culture

Keloid tissues were obtained from five different Japanese patients and normal skin sample was obtained from one Japanese patient by surgical excision after obtaining informed consent, in compliance with the ethical guidelines of Sapporo Medical University School of Medicine. All keloid tissue specimens were pathologically examined to confirm the diagnosis. None of the patients had received previous treatment and had complicating disease that might affect wound healing such as diabetes mellitus. The normal skin sample was obtained by surgery from the nonkeloid patient. Their detailed information is listed in Table 1. After the keloid lesions were resected, full-thickness biopsy specimens were obtained from elevated and red regions (peripheral parts) and shrunken and soft regions (central parts) of each keloid lesion. Explant culture of fibroblasts was performed. A small amount of tissue was dissected free of fat and minced into pieces smaller than 1 mm in diameter. Explants were maintained in DMEM supplemented with 10% FBS in a 5% CO_2 humidified atmosphere at 37 °C. The medium was changed every 2–3 days. Seven to 14 days after the primary culture, cells that proliferated from the edge of the explanted tissue were passaged. The keloid fibroblasts in passages 2–5 were used for all experiments. Fibroblasts harvested from the central keloid area were designated central keloid fibroblasts and those from peripheral areas were designated peripheral keloid fibroblasts.

Reverse transcription-polymerase chain reaction (PCR)

Keloid fibroblasts and normal skin fibroblasts (2×10^3 cell/cm^2) were plated in 100 mm dishes in medium containing 10% FBS. After incubation for 24 hours, the medium was changed with serum-free medium containing resveratrol (0, 25, 50, or 100 μM) and incubated for 48 hours. The cells were trypsinized, counted to make up the cell number and pelleted by centrifugation. The total RNA of pretreated cells was extracted using an RNeasy Mini Kit (Qiagen, Tokyo, Japan) according to the manufacturer's instructions. Reverse transcription was carried out using 2 μg of total RNA as a template with Superscript III Reverse Transcriptase (Invitrogen) according to the manufacturer's instructions. PCR was performed using taq DNA Polymerase (Qiagen) and specific primers (Table 2). Samples were incubated in a PCR thermal cycler (Gene Amp, Life Technologies Japan, Tokyo, Japan). The thermal profile consisted of denaturation at 94 °C for 15 seconds, annealing at 60 °C for 30 seconds and extension at 72 °C for 30 seconds, for 30 cycles. Amplified products (15 μL) were loaded onto a 2% agarose gel in tris-acetate-ethylenediaminetetraacetic acid (TAE) buffer, and separated bands were visualized by ethidium bromide staining. The relative densities of bands were quantified using Dolphin-View (Kurabo, Osaka, Japan).

Western blotting analysis

Keloid fibroblasts (1×10^4 cell/cm^2) were plated in 6-well plates in medium containing 10% FBS. After incubation for 24 hours, the medium was changed with serum-free medium containing resveratrol (0, 25, 50, or 100 μM) and incubated for 48 hours. Cells were lysed as previously described. The extraction of whole cell proteins were run on 10% sodium dodecylsulfate-polyaclylamidegel electrophoresis (SDS-PAGE) gels and electrophoretically transferred to nitrocellulose membranes. These were then soaked in blocking buffer (5% skimmed milk and 0.1% Tween 20 in phosphate-buffered saline [PBS], pH 7.4) for 30 minutes at room temperature and incubated with the primary antibodies for 1 hour at room temperature. The following antibodies were used for Western blot: mouse anti-HSP47 (1 : 1000) (Santa Cruz Biotechnology, Inc., Heidelberg, Germany), and mouse anti-beta-actin (1 : 1000) (Sigma-Aldrich, St Louis, MO). Immunoreactivity

Table 2. Primer sequences for PCR

Target gene	Primer sequence
Type I collagen	(F) 5′-CCCTGGAAAGAATGGAGATG-3′
	(R) 5′-AGCACCAGTGTCTCCTTTGC-3′
α-SMA	(F) 5′-CAACCGGGAGAAAATGACTC-3′
	(R) 5′-CATGGATGCCAGCAGACTC-3′
HSP47	(F) 5′-GCGGGCTAAGAGTAGAATCG-3′
	(R) 5′-AGGACCGAGTCACCATGAAG-3′
G3PDH	(F) 5′-TCCACCACCCTGTTGCTGTA-3′
	(R) 5′-ACCACAGTCCATGCCATCAC-3′

G3PDH, glyceraldehyde-3-phosphate dehydrogenase.

was detected by sequential incubation with a goat peroxidase-conjugated secondary antibody and ECL Western Blotting Detection System (GE Healthcare, UK, Ltd., Buckinghamshire, United Kingdom).

WST-1 assay

Cell suspensions were added to each well of 96-well flat-bottomed microtiter plates (1×10^3 per well) in quintuplicate with 100 μL of medium containing 10% FBS and incubated for 24 hours before treatment with resveratrol. The medium was changed with serum-free medium, and solutions of resveratrol were added to each well at the concentration of 0, 25, 50, or 100 μM. After 12, 24, 36, and 48 hours exposure to the resveratrol, 10 μL of water soluble tetrazolium salts (WST-1) solution (Dojindo Laboratories, Kumamoto, Japan) was added to each well and incubated for 1 hour at 37°C. Optical densities were measured at 450 nm in a microtiter plate reader (ARVO SX, PerkinElmer, Inc., MA).

Enzyme-linked immunosorbent assay

Keloid fibroblasts (1×10^4 cell/cm^2) were plated in 96-well dish in triplicate with 100 μL of medium containing 10% FBS and incubated for 24 hours. The medium was changed with serum-free medium containing resveratrol (0, 25, 50, or 100 μM) and incubated for 48 hours. Treated cell culture supernatants were collected in sterile test tubes. The TGF-β1 concentrations were determined by an enzyme-linked immunosorbent assay (ELISA) technique (R&D Systems, Minneapolis, MN). Total TGF-β1 levels were assayed using a commercial ELISA according to the manufacturer's instructions (R&D Systems).

Caspase-3 activity assay

Keloid fibroblasts (2×10^3 cell/cm^2) were plated in 100 mm dishes in medium containing 10% FBS. After incubation for 24 hours, the medium was changed with serum-free medium containing resveratrol (0, 25, 50, or 100 μM) and incubated for 8 hours. The levels of caspase activities in treated keloid fibroblasts were determined using a commercial fluorometric assay kit (Caspase Colorimetric Protease Assay Kit; MBL, Nagoya, Japan), according to the manufacturer's instructions.[16] In this fluorometric assay, caspase-3 activities were measured by cleavage of the fluorometric substrate DEVD-pNA (Asp-Glu-Val-Asp-p-nitroaniline). Cells including the detached cells were collected and lysed. Then lysates were centrifuged and cleared supernatants were collected. The supernatants were incubated with DEVE-pNA at 37°C for 1 hour. Optical density for each specimen was determined at 405 nm using a plate reader (ARVO SX, PerkinElmer, Inc.).

Annexin-V assay

Keloid fibroblasts (2×10^3 cell/cm^2) were plated in 75 cm^2 flasks in medium containing 10% FBS. After incubation for 24 hours, the medium was changed with serum-free medium containing resveratrol (100 μM) and incubated for 48 hours. At the end of the incubation period, cells were harvested using 0.02% EDTA solution and washed with PBS. Afterward, apoptotic cells were determined by using Annexin-V-Fluos and staining (Annexin-V-FLUOS Staining Kit, Roche Diagnostics K. K., Tokyo, Japan) according to the manufacturer's instructions. Labeled cells were then counted on a FACSCalibur flow cytometer (Becton Dickinson, Franklin Lakes, NJ).

Cell cycle analysis

To investigate the cell cycle distribution patterns of resveratrol-treated fibroblasts, we used flow cytometry to observe the cell cycle distribution. Keloid fibroblasts (2×10^5 cell/cm^2) were plated in 75 cm^2 flasks in medium containing 10% FBS. After incubation for 24 hours, the medium was changed with serum-free medium containing resveratrol (100 μM) and incubated for 48 hours. Then the cells were harvested with 0.02% EDTA solution, washed and collected. The fibroblasts were fixed in 75% (v/v) cold ethanol at −20 °C for at least 1 hour. The fixed cells were collected by centrifugation and resuspended in RNase Staining Buffer (Phoenix Flow Systems, San Diego, CA) to stain DNA and finally analyzed on a FACSCalibur flow cytometer (Becton Dickinson, NJ, USA). Cell cycle distribution of keloid-derived fibroblasts was analyzed on a FACSCalibur flow cytometer. Cell cycle distribution was calculated using the Cell Quest software program (Becton Dickinson). The percentages of cells in the G0/G1, G2/M, S, and sub-G1 phases of the cell cycle were autoanalyzed using the supplied ModFit LT software program (Verity Software House, Topsham, ME). Data are expressed as the percentages of cells in the G0/G1, G2/M, S, and sub-G1 phases.

Statistical analysis

Data were expressed at means ± standard deviations (SDs) of duplicate experiments carried out for five separate runs. Means of two groups were compared using Student's t test; p-values < 0.05 were considered statistically significant. Densitometric analysis was performed using ImageJ, a Java program developed by National Institutes of Health (NIH; Bethedsa, MD).

RESULTS

Resveratrol suppressed the expression of type I collagen, α-SMA, and HSP47 of keloid fibroblasts

The effect of resveratrol on type I collagen and α-SMA mRNA expression of keloid fibroblasts was investigated first. The mRNA expression of type I collagen and α-SMA decreased in keloid fibroblasts in a dose-dependent manner (Figure 1A and B). HSP47 is a collagen-specific molecular chaperone that is elevated in parallel with collagen expression in fibrotic disorders, including keloids.[17,18] Resveratrol treatment showed an inhibitory effect on HSP47 mRNA expression similar to that type I collagen and α-SMA(Figure 1A and B). We then examined protein expression levels of HSP47 by Western blot analysis. It showed that resveratrol decreased HSP47 expression in a dose-dependent manner (Figure 1C and D). The suppression was obvious at day 2 after resveratrol

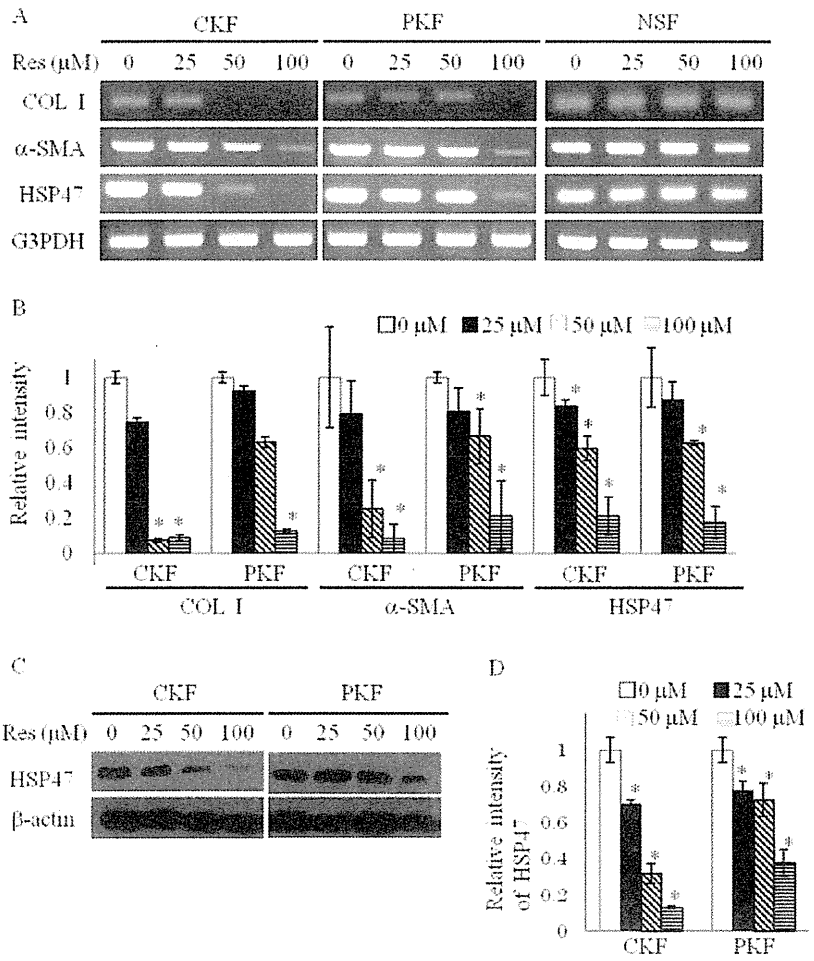

Figure 1. Effect of resveratrol on type I collagen, α-SMA, and HSP47 mRNA expression of keloid fibroblasts and normal fibroblasts. (A) Representative image of type I collagen, α-SMA, and HSP47 mRNA expression in keloid fibroblasts, third passage from patient 1 (31-year-old woman, pubic region), and normal fibroblasts, third passage from patient 6 (25-year-old woman, ear), after 48 hours exposure to resveratrol (0, 25, 50, 100 μM). (B) Results of densitometric analysis of detected bands by RT-PCR. Relative intensity of type I collagen, α-SMA, and HSP47 mRNA expression after scanning densitometry and normalization to G3PDH expression, respectively. Results are expressed as relative levels compared with those of untreated cells (0 μM resveratrol). Data are presented as mean ± SD of five different samples (patients 1–5 described in Table 1). $*p < 0.05$ compared with control levels. (C) Representative blot image of expression of HSP47 and β-cytoplasmic actin analyzed by Western blot. (D) Results of densitometric analysis of detected bands by Western blot. The relative intensity ratio of the two bands of HSP and β-actin in control cells (0 μM resveratrol) was arbitrarily set as 1. Data are presented as mean ± SD of five different samples (patients 1–5 described in Table 1). $*p < 0.05$ compared with control levels. CKF, central keloid fibroblasts; PKF, peripheral keloid fibroblasts; NSF, normal skin fibroblasts; COL I, type I collagen; Res, resveratrol.

treatment. We examined the effect of resveratrol on normal skin fibroblasts in a similar method. However, resveratrol did not decrease type I collagen, α-SMA, and HSP47 mRNA expression in fibroblasts from normal skin (Figure 1A). These results suggested that resveratrol suppressed collagen production of keloid fibroblasts and played an important role to maintain keleoid fibroblasts in the quiescent state.

Resveratrol reduced TGF-β1 production by keloid fibroblasts

TGF-β1 is one of the key mediators of fibrogenesis. It is known to be up-regulated in keloid tissue and to stimulate the proliferation of fibroblasts. It also promotes type I collagen synthesis and inhibits the transcription of collagenase.[19] Therefore, we next performed an assay using a TGF-β1 ELISA kit to quantify the amount of TGF-β1 protein present in the culture supernatant. The results showed resveratrol tend to suppress TGF-β1 production of central keloid fibroblasts, although there is no statistical significant difference. On the other hand, resveratrol, especially in 100μM, significantly suppressed TGF-β1 production of peripheral keloid fibroblasts ($p < 0.05$) (Figure 2).

Resveratrol inhibited the proliferation of keloid fibroblasts and induced apoptosis in keloid fibroblasts

We examined the effect of resveratrol on keloid fibroblast proliferation. Cells were treated with resveratrol at the concentration of 0, 25, 50, or 100 μM and cultured for up to 48 hours (Figure 3). It was shown that resveratrol treatment induced a concentration-dependent reduction in the proliferative activity of keloid fibroblasts. We examined the effect of resveratrol on normal skin fibroblast proliferation. Although resveratrol seems to have a tendency to decrease normal skin fibroblasts proliferation in dose dependent, only with 100 μM showed statistical significant difference (Figure 3A).

We observed that resveratrol-treated cells became round, shrunken, and floating, which are the characteristics of apoptotic cells that were not seen in the untreated controls (Figure 4). To investigate the growth-inhibitory mechanism of resveratrol, two-color staining with annexin-V and propidium iodide was used to detect the fraction of cells undergoing early apoptosis and subsequent cell death. We assessed cell apoptosis only at 48 hours based on our earlier observation of the time course of growth inhibition by resveratrol on keloid

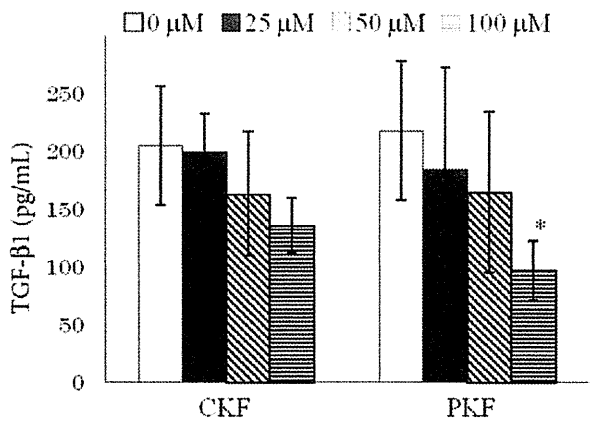

Figure 2. Levels of TGF-β1 in keloid fibroblast culture supernatants. Cells were seeded 3,200 cells/well in 96-well plates in triplicate and treated with resveratrol (0, 25, 50, or 100 μM) for 48 hours, and the supernatants were assayed by ELISA. Data are presented as mean ± SD of five different samples (patients 1–5 described in Table 1). $*p < 0.05$ compared with control (0 μM resveratrol) levels. CKF, central keloid fibroblasts; PKF, peripheral keloid fibroblasts.

fibroblasts. As shown in Figure 5, 100 μM resveratrol induced cell apoptosis in keloid fibroblasts. In central keloid fibroblasts, 18.7% of total cells were induced to undergo early apoptosis, 73.2% late apoptosis, and 7.9% necrosis. In peripheral keloid fibroblasts, 49.7% of total cells were induced to undergo early apoptosis, 19.8% late apoptosis, and 7.1% necrosis (Figure 5A). Next, to understand the effect of resveratrol on cell cycle progression, keloid fibroblasts were treated with 100 μM resveratrol, and the cell cycle was analyzed by flow cytometry. The data are expressed as the percentages of cells in the G0/G1 phase, G2/M phase, S phase, and sub-G1 phase (apoptosis). Both the central and peripheral keloid fibroblasts showed significant increases in the number of apoptotic cells after treatment with 100 μM resveratrol for 48 hours (Figure 5C).

As caspase-3 is known to be a key effecter molecule in the execution of apoptotic stimuli,[20,21] we examined whether resveratrol activated caspase-3 in keloid fibroblasts. We observed that caspase-3 was activated in resveratrol-treated keloid fibroblasts at 8 hours after treatment (Figure 5D). These results suggested that caspase-3 might be activated by resveratrol at an early stage of apoptosis.

DISCUSSION

Today, there is no effective pharmacological treatment for keloids which, characterized by an abundant accumulation of extracellular matrix, are benign collagenous tumors that occur during abnormal wound healing. It has been reported that the growth potential of keloid fibroblasts could be higher than that of normal skin fibroblasts, and keloid fibroblasts are resistant to apoptosis induced by several stimuli such as antitumor necrosis factor receptor superfamily, member 6 (Fas) antibodies, staurosporin, and C2 ceramide.[8,22] Apoptosis could mediate the transition from the granulation phase to the normal scar in the wound healing process. These findings suggest that keloid formation could be a result of an abnormal wound healing process with prolonged cell growth and resistance to apoptosis, with subsequent collagen accumulation. Resveratrol has been reported to exhibit antifibrogenic effects through a variety of mechanisms;[23,24] however, its effects on keloids are not clearly established. We investigated whether resveratrol could be effective against keloid fibroblasts on collagen production, cell growth, and apoptosis.

We examined, first of all, the effect of resveratrol on the expression of type I collagen, which is a major component of the extracelluar matrix. Its overexpression is one of the pathophysiological characteristics of keloid formation. α-SMA is thought to be one of the most useful markers for myofibroblast phenotype. Our results showed that resveratrol inhibited the expression of type I collagen and α-SMA mRNA in a dose-dependent manner. It has been described that collagen synthesis is higher in peripheral keloid fibroblasts compared with central keloid fibroblasts.[25] In our study, peripheral keloid fibroblasts treated with 50 μM of resveratrol expressed type I collagen mRNA unlike in the case of central keloid fibroblasts. From that result, peripheral keloid fibroblasts might be relatively resistant to resveratrol than central keloid

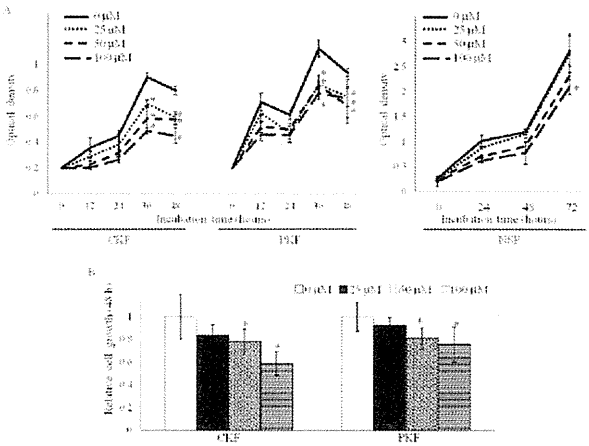

Figure 3. Effect of resveratrol on cell growth. (A) Representative cell growth carves of keloid fibroblasts, second passage from patient 2 (48-year-old woman, shoulder), and normal skin fibroblasts, third passage from patient 6 (25-year-old woman, ear). Cells were plated 320 cells/well in 96-well plates and treated with resveratrol (0, 25, 50, or 100 μM) and cultured for up to 48 hours. Treated cells were estimated by WST-1 assay. Each point indicates the mean ± SD of the data collected from three wells. $*p < 0.05$ compared with control (0 μM resveratrol). (B) Relative cell number at 48 hours. Results are expressed as relative levels compared to those of untreated cells (0 μM resveratrol). Data are presented as mean ± SD of five different samples (patients 1–5 described in Table 1). $*p < 0.05$ compared with control (resveratol 0 μM). Each point indicates the mean ± SD of the data collected from three wells. $*p < 0.05$ compared with control (resveratol 0 μM). CKF, central keloid fibroblasts; PKF, peripheral keloid fibroblasts; NSF, normal skin fibroblasts.